

# Chapter 5

## FT-IR Characterization

IR spectroscopy is a technique that is commonly used to characterize materials. Of the different modalities, transmission-absorption, diffuse reflectance and attenuated total reflection are the most frequent.

The IR spectroscopic study of surface active centers is based on the observation that vibrational perturbation undergoes by probe-molecules when they adsorb on the surface.

The ideal probe molecule should have certain characteristics:

- The functional group or the atom through which the molecule is bonded to the surface should be well known.
- The probe molecules should form the same interaction complex for similar adsorbents.
- Adsorption complexes should be stable enough to allow characterization.
- The probe molecules should have spectral parameters that are sensitive to the state of the sites on which they are adsorbed.
- The informative absorption bands of the complexes should be in regions in which the sample is transparent.
- The extinction coefficients of the informative bands must be high.
- The probe molecule should not cause any chemical modification to the surface.

- The probe molecule should be small enough to avoid steric hindrance of the adsorption.

Because we were studying cations or Brønsted acid type centres, we used nitriles of different sizes and electronic properties, and CO to characterize the zeolite samples.

Nitriles are relatively weak bases and coordinate via the nitrogen of the nitrile group to the acid sites. Upon interaction, the band of the CN stretching vibration is shifted to higher wavenumbers. Coordination to aprotic sites via the nitrogen lone-pair electrons results in blue shifts of approximately 30 to 60  $\text{cm}^{-1}$ . Coordination to a hydroxyl group, on the other hand, results in shifts of approximately 10 to 30  $\text{cm}^{-1}$ .

Carbon monoxide is a weak base molecule and interactions with most solid acids are weak. Thus, low temperature adsorption experiments are necessary for more quantitative studies. Under these conditions, CO is unreactive for all practical purposes, and Brønsted and Lewis sites can be qualitatively and quantitatively determined. The smallness of CO makes it possible to probe nearly all acid sites. CO usually interacts by bonding via the carbon atom to the acid sites and shifts the adsorption maximum of the CO stretching vibration band to higher wavenumbers. However, it can also interact by bonding via the oxygen atom to form isocarbonyls, and the result is that the complexes are less stable than the carbon bonded CO. In this case the CO stretching frequency shifts to lower frequencies. In addition, other complexes for example, with CO in bridging position, CO bonded via both ends or species like  $\text{M}^{n+}(\text{CO})_x$ , can also be found.

In our work, adsorption experiments were first performed on Na-Mordenite (chapter 5.1) in order to characterize its active sites, and a new interaction was found with either nitriles or CO adsorption. Therefore, in order to go more

deeply into this interaction, these probe molecules were adsorbed into several alkali-mordenites (chapter 5.2) and on two sodium faujasites (chapter 5.3).

## 5.1. An FT-IR study of the adsorption of CO and nitriles on Na- Morденite: evidence of a new interaction\*

### *Abstract*

The low-temperature adsorption of CO and the room temperature adsorption of acetonitrile, propionitrile, isobutyronitrile, pivalonitrile, benzonitrile and orthotoluonitrile on Na-mordenite have been investigated by FT-IR spectroscopy. The results have been compared with analogous experiments performed on H-mordenite, Na-X zeolite and Na-silica-alumina. The Na distribution in Na MOR has also been investigated by XRD and Far-IR spectroscopy. The conclusions are that Na ions distribution is essentially random and that together with the well known interaction of the probes with Na ions in the side pockets and the main channels, a stronger additional interaction occurs in all cases. This new interaction is likely multiple, involving either more Na ions or Na and oxygen species. This interaction is more pronounced with the hindered nitriles, whose access at the cavities is likely forbidden. This suggests that this interaction, which is also observed on Na-X zeolites but not with Na-silica-alumina, occurs at the mouths of the mordenite channels.

---

\* Journal of Physical Chemistry B **2005**, 109 (2), 915-922.

### ***5.1.1. Introduction***

Zeolites in their protonic forms are largely used as environmentally friendly catalysts for proton catalyzed reactions.<sup>1</sup> In particular, H-mordenite finds application for catalyzing efficiently the skeletal isomerizations of light alkanes such as butane and pentane.<sup>2</sup> Partially Na-exchanged MOR (Na-H-MOR) has been studied for application in xylenes isomerization.<sup>3</sup> However, usually light alkali metal exchanged zeolites (like e.g. Na-X and Na-Y) act as quite mild basic catalysts.<sup>4-6</sup> Whereas, heavy-alkali metal zeolites (like Cs-Y) are reported to be strong bases. In parallel, Na-zeolites show a mild Lewis acid behavior associated to the activity of highly unsaturated alkali cations which can adsorb electron rich molecules so allowing their separation.<sup>7</sup> Several studies have been reported recently concerning Na-Mordenites. In particular, the effect of localization of Na cations and of hydrations have been studied by dielectric relaxation spectroscopy,<sup>8</sup> by thermally stimulated current measurement<sup>9</sup> and by modelling.<sup>10</sup> The adsorption isotherms of small molecules such as N<sub>2</sub>, H<sub>2</sub> and O<sub>2</sub> have been studied on Na mordenite<sup>11,12</sup> and modified Na mordenites.<sup>13</sup>

The low temperature adsorption of CO is today perhaps the most popular technique for characterizing adsorption sites of zeolites by IR spectroscopy. It actually allows a very detailed analysis of the surface sites as they appear at low temperature without strong perturbations of the surface, having also free access to any cavity and avoiding steric hindrances.<sup>14, 15</sup> This is a good opportunity to evaluate “pure acidity” without any steric constraint,<sup>16</sup> and has been applied to both H-MOR and Na-MOR.<sup>17, 18</sup> On the contrary, the adsorption of a set of differently hindered nitriles allowed to investigate the accessibility and the multiplicity of the protonic sites on H- mordenite<sup>19, 20</sup> and of Cobalt-exchanged mordenite.<sup>21</sup>

In this paper we describe the results of an IR study of the adsorption of different hindered nitriles on Na-mordenite. The results will be compared with those of low temperature CO adsorption measurements. The aim is to have indications on the locations and accessibility of the adsorption sites of Na Mordenite.

## ***5.1.2. Experimental***

### ***5.1.2.1. Sample preparation***

Mordenite has been used as the main object of study of this work.

Na-MOR (Si/Al = 6.5, CBV 10A Lot No. 1822-50) was supplied by Zeolyst as hydrated powder. The chemical composition was SiO<sub>2</sub>/Al<sub>2</sub>O<sub>3</sub> mole ratio 13 and a Na<sub>2</sub>O weight % of 6.6. H-MOR was prepared by cation exchanging the starting form, Na-MOR, with a NH<sub>4</sub>Cl 2.2 M solution and later calcining at 673 K for 12 hours.

Other materials (NaX and Na-Silica-alumina) have also been used in other to clarify some results obtained with mordenite for comparison. NaX zeolite was supplied by Rhône Poulenc. Na-Silica-alumina was prepared by impregnation of a commercial silica–alumina from STREM with a Na<sub>2</sub>CO<sub>3</sub> solution. The impregnation was carried out in order to achieve that the moles of Na<sup>+</sup> ions introduced were equal to the moles of aluminium atoms in the commercial silica-alumina.

### 5.1.2.2. Characterization techniques

Mordenite samples were characterized using the following techniques:

Powder X-ray diffraction patterns of the samples were obtained with a Siemens D5000 diffractometer (Bragg-Brentano parafocusing geometry and vertical  $\theta$ - $\theta$  goniometer) fitted with a curved graphite diffracted-beam monochromator, incident and diffracted-beam Soller slits, a  $0.006^\circ$  receiving slit and scintillation counter as a detector. The angular  $2\theta$  diffraction range was between  $5^\circ$  to  $70^\circ$ . The data were collected with an angular step of  $0.05^\circ$  at 3s per step and sample rotation.  $\text{CuK}\alpha$  (1.542 Å) radiation was obtained from a copper X-ray tube operated at 40kV and 30mA. The cell parameters and cell volume values were calculated using a matching profile with TOPAS 2.0 software (Bruker AXS).

Skeletal MIR (KBr pressed disks) and FIR (pure powder on polyethylene supports) spectra were recorded on a Nicolet Magna 750 Fourier Transform instrument (resolution  $4\text{ cm}^{-1}$ ). Additionally, both samples were characterized (on MIR range) by adsorbing several probe molecules. Different nitriles like acetonitrile (AN), propionitrile (PrN), isobutylonitrile (IBN), pivalonitrile (PN), benzonitrile (BN) and o-toluenitrile (o-TN) were used to characterize mordenite samples, and furthermore CO at low temperature was also used. The pressed disks of pure zeolite powders were activated “in situ” the IR cell by outgassing at 773 K before the adsorption experiments. A conventional gas manipulation/outgassing ramp connected to the IR cell was used.

The adsorption/desorption process has been studied by transmission FT-IR. For nitriles, the adsorption procedure involves contact of the activated sample disk with vapors at room temperature at a pressure not higher than 2,5 kPa. The desorption process at increasing temperatures was performed in vacuum at temperatures compressed in the range 273 K and 573 K. On the other hand, CO adsorption was performed at 130 K by the introduction of a well-known

dose of the gas inside the low temperature infrared cell containing the previously activated wafers. IR spectra were collected evacuating at increasing temperatures between 130 and 273 K. Additionally, the co-adsorption of acetonitrile and CO was performed in the way that first acetonitrile was adsorbed at room temperature and posterior evacuated at 373 K. Consecutively the cell temperature was decreased until 130 K and a well-known dose of CO was introduced, which was posterior evacuated at temperatures between 130 K and 273 K.

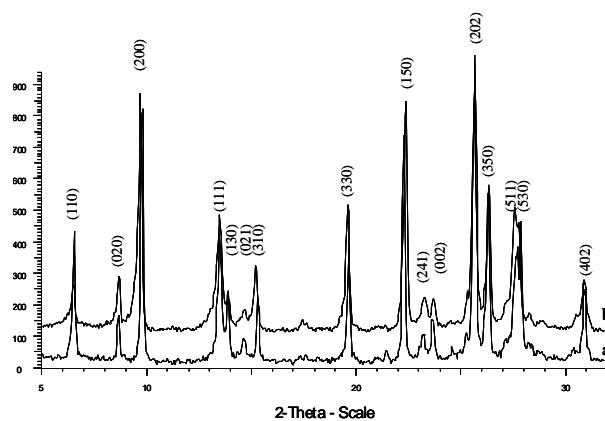
### ***5.1.3. Results and Discussion***

#### ***5.1.3.1. Skeletal MIR and FIR spectra***

Figure 1 shows the X-ray Diffraction patterns obtained for NaMOR and HMOR samples, which agree to the respective Mordenite JCPDS file. The calculated cell parameters and cell volume for both samples are also reported in Table 1. Both samples present similar cristallinity, and no significant differences on the peak width and on the peak intensity are appreciable from X-ray patterns in Figure 1. However, the cell parameters values indicate an increase on the cell dimensions from HMOR to NaMOR, which can be assigned to the effect of the different dimensions of H<sup>+</sup> and Na<sup>+</sup> cations in the cavities and to a certain dealumination during HMOR preparation. In both NaMOR and HMOR X-ray patterns only hkl peaks assigned to the Mordenite framework can be observed. Consequently, the absence of hkl peaks associated to a cation match on structure, suggest that cations may be randomly distributed on mordenite.

**Table 1.** Cell parameters of HMOR and NaMOR samples calculated by XRD.

Sample	a (Å)	b (Å)	c (Å)	cell vol. (Å <sup>3</sup> )
HMOR	18.098(4)	20.447(3)	7.510(1)	2279
NaMOR	18.180(4)	20.315(3)	7.484(1)	2764

**Figure 1.** X-ray Diffraction patterns of NaMOR (a) and HMOR (b) samples.

In Figure 2, the skeletal IR spectra (KBr pressed disks) for HMOR and NaMOR are reported. The spectra compare well with those reported in the literature. The substitution of Na<sup>+</sup> cations for H<sup>+</sup> causes a slight shift to higher frequencies of the main maximum in the massive asymmetric mode probably related to some dealumination in the preparation process<sup>22</sup>. Also in FIR spectra no differences associated to the cation type present can be distinguished in both samples. In particular no bands are observed in the region below 450 cm<sup>-1</sup>, where Na-oxygen stretching modes are expected and found e.g. in the case of

NaX zeolite.<sup>22</sup> This fact agrees with a random distribution of Na<sup>+</sup> cations in the structure.

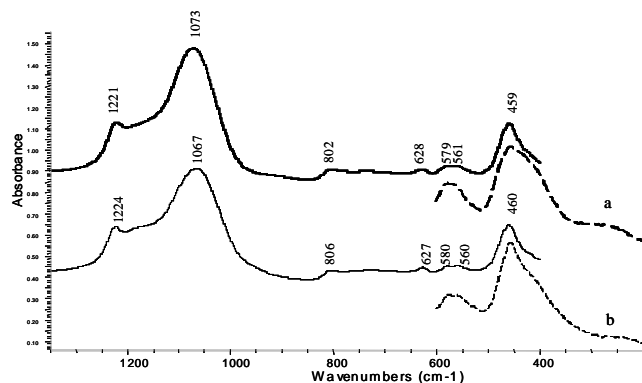


**Figure 2.** Skeletal MIR (continuous line) and FIR (discontinuous line) of HMOR (a) and NaMOR (b) samples.

### 5.1.3.2. Spectra of the surface hydroxy groups

The overall spectrum of activated Na-MOR sample (pure powder pressed disks) in the 4000-900 cm<sup>-1</sup> range is compared to the spectrum of H-MOR sample in Figure 3. In the OH stretching region for HMOR sample, two bands can be observed: the first at 3744 cm<sup>-1</sup> associated to the terminal silanol groups, and the second one (very strong and complex) with the main maximum at 3605 cm<sup>-1</sup>, assigned to the bridging Si-OH-Al groups. According to Bevilacqua et al. such OH groups are exclusively located on the inner surface and possess a strong Brønsted acidity.<sup>19,20</sup> The asymmetry of this band indicates the presence of different components. At least three components were previously identified by Bevilacqua et al.<sup>19,20</sup> and later confirmed by Marie et al.<sup>17</sup> An additional weak component can be observed for HMOR sample at 3655 cm<sup>-1</sup>, which can be

associated to small amounts of extraframework aluminum species formed during the activation by heating *in vacuo*. Meanwhile for Na-MOR, only one small peak at  $3745\text{ cm}^{-1}$  was observed. The absence of the band centred at  $3605\text{ cm}^{-1}$  indicates that all the possible cationic positions are occupied by  $\text{Na}^+$  cations in the Na-MOR sample. In contrast, the band corresponding to terminal silanol groups has roughly the same intensity and position in both samples, suggesting that external silanols are not affected by cation exchange.

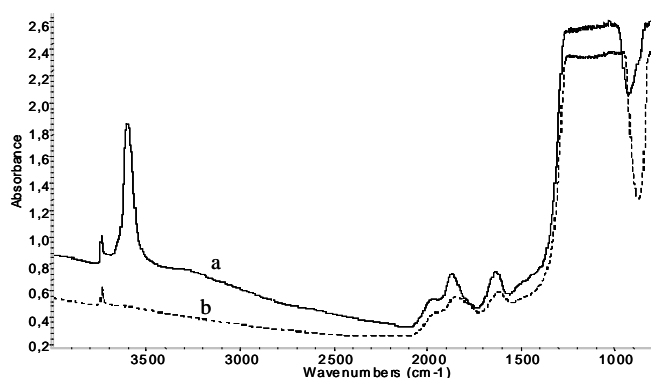


**Figure 3.** FT-IR spectra of activated HMOR (a) and NaMOR (b) samples at 773 K in vacuum conditions.

In the  $2100\text{--}1500\text{ cm}^{-1}$  region, three typical skeletal overtones are found like on any silica-based material, while in the region between  $1300$  and  $1000\text{ cm}^{-1}$  a cut-off is observed due to the Si-O-Si(Al) asymmetric stretching skeletal mode. In agreement with the shift observed for the main maximum near  $1070\text{ cm}^{-1}$  in the skeletal spectrum (KBr disks), also in the pure powder pressed disks spectrum, both overtones and fundamental skeletal bands are slightly shifted to lower frequencies for NaMOR respect to HMOR.

### ***5.1.3.3. Low temperature adsorption of CO on NaMOR and HMOR***

Adsorption of CO at low temperature has been carried out on both zeolites (Figures 4, 5 and 6). Figure 4 shows the IR bands of adsorbed CO on NaMOR. At 133 K (real adsorption temperature as measured on the sample when liquid nitrogen is in the external cooling jacket) two main bands are observed on the CO stretching range: the first one, more intense, has the main maximum at 2164  $\text{cm}^{-1}$  and a shoulder at 2175  $\text{cm}^{-1}$  and the second one, less intense, located at 2138  $\text{cm}^{-1}$ . By progressively increasing temperature upon outgassing, the higher frequency band together with its shoulder parallelly decrease their intensity. In the same way, the lower frequency band decreases on intensity, but much slower, when temperature increases. However, this band, which is initially weaker than the higher frequency band, has finally a similar intensity at 213 K and 233 K. In the OH vibration range (not shown here), the band at 3745  $\text{cm}^{-1}$  is not perturbed indicating that terminal silanol groups do not interact with CO molecules in these conditions.

The band at 2164  $\text{cm}^{-1}$  with its shoulder at 2175  $\text{cm}^{-1}$  have been previously identified by other authors. Marie et al. have found them at 2163 and 2174  $\text{cm}^{-1}$  for a NaMOR (Si/Al ratio 10).<sup>17</sup> Bordiga et al. reported the frequency of those bands at 2159 and 2177  $\text{cm}^{-1}$  for a NaMOR (Si/Al of 5).<sup>18</sup> In both papers, taking into account the respective polarizing properties of cations depending on the location in the zeolitic structure, the component at lower frequency has been assigned to the C-bonded CO interacting with  $\text{Na}^+$  cations located on the side pockets, while the component at higher frequency has been associated to the CO interacting with those located on the main channels.

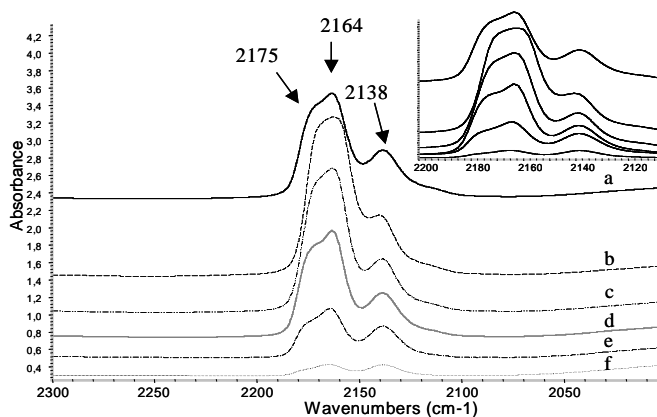


**Figure 4.** FT-IR spectra of NaMOR in the presence of CO gas at 133 K (a), and under evacuation at 143 K (b), 173 K (c), 193 K (d), 213 K (e), 233 K (f) on the CO stretching range.

The band at  $2138\text{ cm}^{-1}$  (wavenumber value which is very near to that of liquid CO) can be attributed to pseudo-liquid physisorbed CO inside the zeolite pores with hindered rotation<sup>15,17,18</sup>, which should desorb or evaporate quite fast. However, from our spectra, the intensity of this band decreases slower than that expected for pseudo-liquid physisorbed CO, even slower than those two higher frequency bands. Therefore, this disagrees with the assignment of this band to liquid-like CO only. In our opinion two superposed bands are present. The initial decrease of the band could be due to an evacuation of pseudo-liquid CO, which should be responsible for only part of this band, but the posterior so slow decrease on the intensity can evidence the existence of an additional stronger interaction-like involving  $\text{Na}^+$  cations. This interaction cannot be apparently attributed to O-bonded CO species ( $\text{Na}^+ \cdots \text{OC}$ ) since this interaction has been reported to absorb at lower frequencies (between  $2220$  and  $2212\text{ cm}^{-1}$ ).<sup>15,23</sup> The possibility of the formation of CO species interacting with two  $\text{Na}^+$  ions will be discussed below.

The adsorption of CO on HMOR gives rise, on the CO stretching range, again to two bands: one, the first formed and last disappeared during outgassing, centred at 2173  $\text{cm}^{-1}$  with a tail towards lower frequencies, and the other one, again at 2138  $\text{cm}^{-1}$  (Figure 5). In that case, contrarily to that observed for NaMOR, we are unable to single out two components for CO stretching band of C-bonded CO interacting with  $\text{H}^+$  located on the main channels and side pockets. In that case, the band at 2138  $\text{cm}^{-1}$  disappears progressively upon outgassing and can consequently be assigned, with confidence, to the pseudo-liquid CO. This further supports the idea that part of the band at 2138  $\text{cm}^{-1}$  on NaMOR is something associated to interactions of CO molecules with  $\text{Na}^+$  cations.

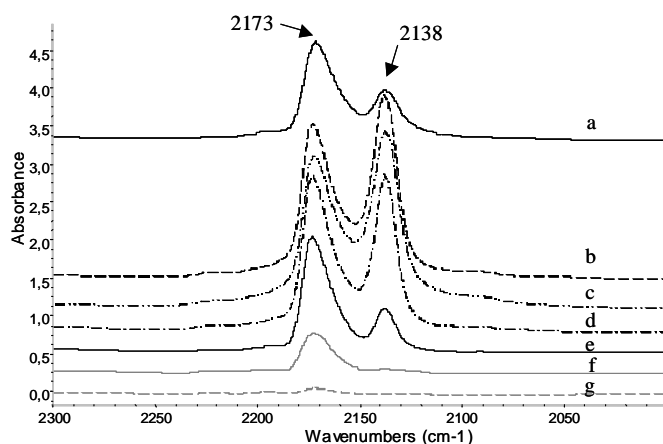


**Figure 5.** FT-IR spectra of HMOR in the presence of CO gas taken immediately at 133 K (a) and after 2 min (b), and under evacuation at 133 K (c), 143 K (d), 173 K (e), 193 (f) and 213K (g) on the CO stretching range.

Figure 6 shows the effects of the CO adsorption on HMOR in the OH vibration range. The band at 3745  $\text{cm}^{-1}$  is not perturbed as for the NaMOR sample. Otherwise, just after contacting surface with CO (Figure 6a) only part

of the bridging OH band at  $3605\text{ cm}^{-1}$  shifts to near  $3300\text{ cm}^{-1}$ , and a residual band is still present at  $3590\text{ cm}^{-1}$ . After more prolonged contact, this component at  $3590\text{ cm}^{-1}$  disappears and the band of the OH, interacting with CO, seems to present an additional component at higher frequencies (around  $3400\text{ cm}^{-1}$ ). By evacuating, the situation seems to be exactly reversed, since, in first place, the component near  $3590\text{ cm}^{-1}$  is restored, when the absorption near  $3400\text{ cm}^{-1}$  disappears, while the band at  $3605\text{ cm}^{-1}$  is restored later. Our conclusion is that CO adsorbs first on OHs in the main channels and later, more slowly, diffuses into the side pockets. The OHs located in the side pockets, responsible for the  $3590\text{ cm}^{-1}$  band, are less perturbed than those in the main channels upon interaction with CO. This may be due to a higher acidity of OHs in the main channels or to some hindering of the interaction occurring in the side pockets in agreement with Hadjiivanov et al.<sup>15</sup> and Maache et al.<sup>24</sup>

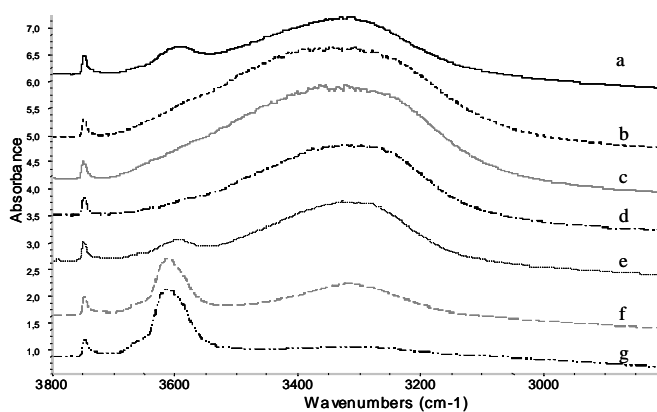


**Figure 6.** FT-IR spectra of HMOR in the presence of CO gas taken immediately at 133 K (a) and after 2 minutes (b), and under evacuation at 133 K (c), 143 K (d), 173 K (e), 193 (f) and 213K (g) on the OH vibration range.

#### ***5.1.3.4. IR study of the adsorption of acetonitrile and propionitrile***

Acetonitrile (AN) adsorption has been used for characterizing the different hydroxy groups of H-zeolites including HMOR, since they can access to all protonic sites on HMOR.<sup>19,25</sup> The AN adsorption has also been investigated on NaY and NaX.<sup>26, 27</sup>

The spectra of AN adsorbed on NaMOR sample, and after outgassing at different temperatures are shown in Figure 7. The activated sample spectrum as well as the gas phase spectrum have been subtracted to all spectra. The same procedure has been applied to all adsorption experiments reported in this work. The nitrile spectrum on CCl<sub>4</sub> solution, used as a reference, is also shown.

From the subtracted spectra obtained in contact with AN vapour and evacuated at room temperature (Figure 7b-7c) two bands at 2268 cm<sup>-1</sup> and 2299 cm<sup>-1</sup> can be observed on the CN stretching region. It is well known that the AN CN stretching mode gives place to two bands due to the Fermi Resonance between the fundamental stretching CN with a  $\delta\text{CH}_3 + \nu\text{C-C}$  combination. Both bands are slightly asymmetric with a tail towards lower frequencies. By evacuating, the bands become narrower since the tail at lower frequencies seems to disappear. On the desorption process, by increasing temperature under vacuum, the intensity of these bands on the CN region decreases, and additionally, when outgassing at 373 K and 473 K (Figure 7d-7e) a new band at 2248 cm<sup>-1</sup> is also observed, possibly with a further Fermi Resonance component near 2270 cm<sup>-1</sup>. The position of the main CN Fermi Resonance bands (2268 and 2299 cm<sup>-1</sup>) of adsorbed AN is, as usual, shifted to higher frequencies than those observed in CCl<sub>4</sub> diluted solution. In contrast, the doubled still present after outgassing at 473 K is observed at slightly lower frequencies than in CCl<sub>4</sub> solution.

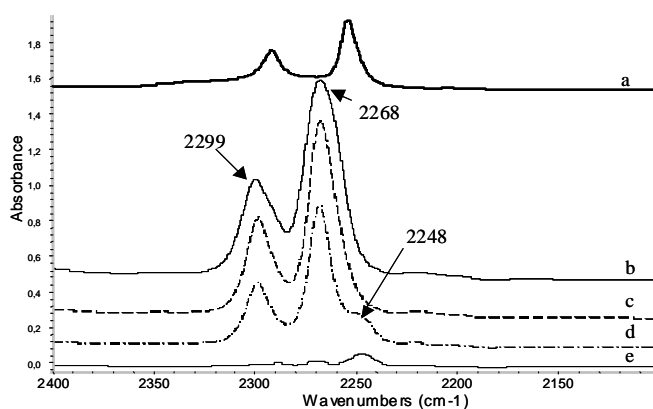


**Figure 7.** FT-IR spectra of AN in CCl<sub>4</sub> solution (a), NaMOR in the presence of AN vapors (b) and after evacuation at room temperature (c), 373 K (d) and 473 K (e).

The subtracted spectra of PrN adsorbed on NaMOR sample and after outgassing at different temperatures are shown in Figure 8. For propionitrile adsorption on NaMOR, one asymmetric band with a maximum at 2267 cm<sup>-1</sup> can be observed on the CN stretching in the presence of PrN vapors. The tail observed towards lower frequencies starts to disappear upon evacuation at room temperature (Figure 8b-8c). By increasing temperature, the band intensity decreases and a new component at 2241 cm<sup>-1</sup> appears at 373 K (Figure 8d-8e). Again the main band is at definitely higher frequency than that observed for the nitrile in CCl<sub>4</sub> solution whereas the band appeared after evacuation at 473 K is at lower frequencies.

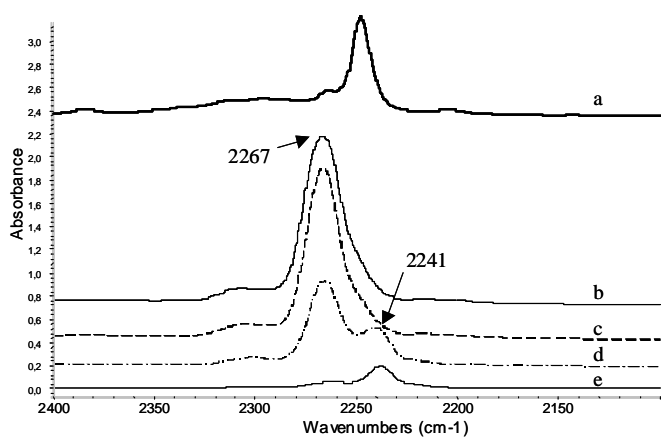


**Figure 8.** FT-IR spectra of PrN in  $\text{CCl}_4$  solution (a), NaMOR in the presence of PrN vapors (b) and after evacuation at room temperature (c), 373 K (d) and 473 K (e).

The main bands at 2268 and 2299  $\text{cm}^{-1}$  observed for AN adsorbed on NaMOR can be assigned to the same interaction of CN group with  $\text{Na}^+$  cations observed for AN adsorbed on NaY (2293 and 2263  $\text{cm}^{-1}$ )<sup>26</sup> and on NaX (2296 and 2267  $\text{cm}^{-1}$ )<sup>27</sup> and also for the  $\text{Na}(\text{CH}_3\text{CN})_3^+$  complex in solution (2302 and 2270  $\text{cm}^{-1}$ ).<sup>27</sup> Moreover, the lower frequency tails observed could be attributed to the CN group interaction with terminal silanol groups since on the OHs region (not shown here) it is clear that the terminal silanol groups are perturbed on contact with nitrile vapors, since the OHs band at 3745  $\text{cm}^{-1}$  disappears, and a broad new band centered around 3450  $\text{cm}^{-1}$  is observed. The easy recovery of the silanol band by outgassing at room temperature together with the CN stretching tails disappearance indicates the weakness of that interaction.

A parallel situation is found for PrN. The main band at 2267  $\text{cm}^{-1}$ , shifted well above the band in  $\text{CCl}_4$  solution, is assigned to the interaction with  $\text{Na}^+$ , while the tail at lower frequencies is assigned to the interaction with external silanols.

The nature of the species responsible for the bands at 2270 and 2248  $\text{cm}^{-1}$  for AN and at 2241  $\text{cm}^{-1}$  for PrN adsorption experiment, is not straightforward. To our knowledge, there is no case in the literature in which an interaction between nitriles and zeolitic sites gives rise to an IR absorption band at lower frequencies than the corresponding band observed for the liquid (Figures 7a and 8a).

Interestingly, this seems to parallel what happens with CO on NaMOR, which also gives rise to a quite strongly adsorbed species characterized by absorbing at slightly lower frequencies than that observed for free CO.

Trying to clarify this phenomenon we studied the adsorption of more hindered nitrile probe molecules.

#### ***5.1.3.5. IR study of the isobutironitrile and pivalonitrile adsorption***

Isobutironitrile (IBN) and pivalonitrile (PN) have been previously used for the different hydroxy groups characterization on HMOR samples.<sup>19,20</sup> It has been shown that because of the higher steric hindrance of the nitrile alkilic group they do not access all the OH groups on HMOR, in particular IBN does not seem to access the side pockets and PN only interacts with OHs pointing to the centre of the main channels.

The subtracted adsorption/desorption spectra obtained for NaMOR sample using isobutironitrile (IBN) and pivalonitrile (PN) vapors as probe molecules are shown in Figures 9 and 10 respectively. The spectra of IBN on NaMOR after the adsorption and evacuation at increasing temperatures are shown in

Figure 9b-9e. In all cases at least two bands with the maximum at 2260 and 2245  $\text{cm}^{-1}$  are observed. Intensity diminishes by increasing outgassing temperature, but interestingly, the band at lower frequencies does it slower. While the position of the band at higher frequencies keeps invariable, the band at lower frequencies furtherly shifts to lower frequencies (until 2235  $\text{cm}^{-1}$ ) when outgassing temperature increases. Another time, this component is at lower frequencies than that in  $\text{CCl}_4$  solution, while the other component is at higher frequencies.

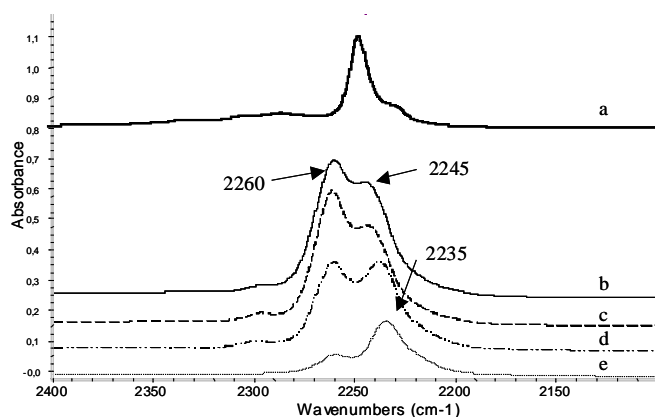


**Figure 9.** FT-IR spectra of IBN in  $\text{CCl}_4$  solution (a), NaMOR in the presence of IBN vapor (b) and after evacuation at room temperature (c), 373 K (d) and 473 K (e).

Adsorption/desorption behaviour observed for PN on NaMOR is similar to that observed for IBN. The spectrum on the CN stretching region obtained at room temperature in the presence of PN vapors shows two bands with the maxima at 2253  $\text{cm}^{-1}$  and 2233  $\text{cm}^{-1}$  (Figure 10b). Again, when temperature increases the bands resolution improves and a decrease on the intensity is also observed. During the desorption process at increasing temperatures (Figure 10c and 10d), as it has been reported above for IBN, a shift is observed for the

lower frequency band, down to  $2221\text{ cm}^{-1}$  at 373 K. Also in that case, that band at lower frequencies shows a higher resistance to the desorption process, since its intensity at 373 K is much more higher than that found for the previously used probe molecules.

In both cases, when NaMOR contacts with nitrile vapours, the band corresponding to the terminal silanol groups (at  $3745\text{ cm}^{-1}$ ) disappears and the previously commented band at  $3450\text{ cm}^{-1}$  is formed. As it was previously commented, silanol-nitrile interaction is weak, since the corresponding OHs band is restored by evacuating at room temperature.

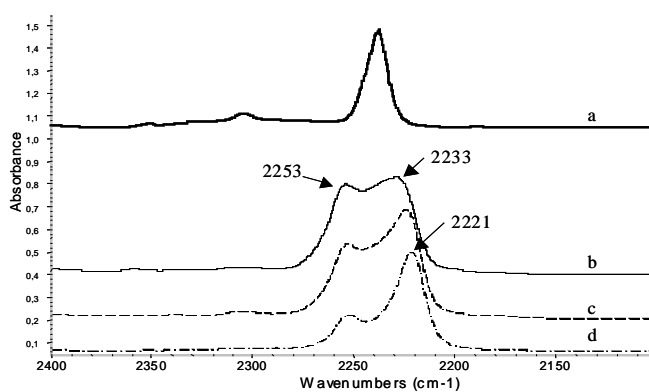


**Figure 10.** FT-IR spectra of PN in  $\text{CCl}_4$  solution (a), NaMOR after evacuation at room (b), at 373 K (c) and 473 K (d).

Interestingly, the highest intensity ratio between the lower and the higher frequency bands was obtained for PN among all the nitriles tested so far. Therefore, in the case of PN, whose access to the channels is highly hindered, the CN stretching band shifted to lower frequencies than the liquid appears to be much stronger than in the case of nitriles with less restricted access to the channels like AN, PrN and IBN.

Due to the fact that the more hindered nitriles give rise to a stronger interaction, additional adsorption studies with other kind of hindered nitriles, as aromatic nitriles, have been performed.

#### **5.1.3.6. IR study of the adsorption of benzonitrile and orthotoluonitrile**

Subtracted spectra of benzonitrile (BN) and orthotoluonitrile (oTN) adsorbed on NaMOR and after evacuation at increasing temperatures are shown in Figure 11 and in Figure 12, respectively. The spectra of the nitriles molecules on NaMOR show in the CN stretching region two peaks, whose main maxima are centred at  $2254\text{ cm}^{-1}$  and  $2221\text{ cm}^{-1}$  for BN and at  $2246$  and  $2216\text{ cm}^{-1}$  for oTN. In both cases, at room temperature, the intensity of the bands at higher frequency is higher than those at lower frequency, but during the desorption process, the intensity of the first ones decreases faster, until they have similar intensity.

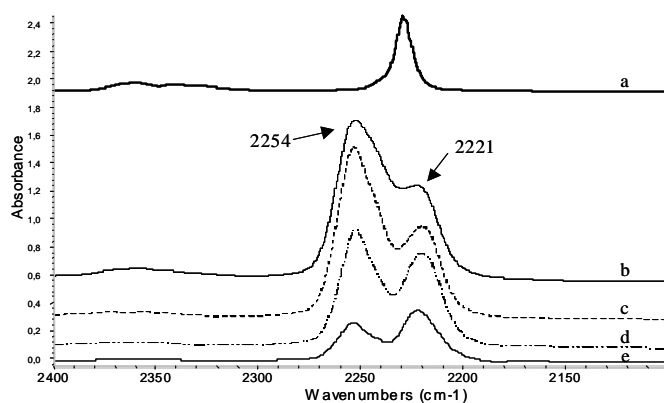


**Figure 11.** FT-IR spectra of liquid BN (a), NaMOR in the presence of BN vapor (b) and after evacuation at room temperature (c), 373 K (d) and 473 K (e).

Comparing those frequencies with that of the nitrile spectra in  $\text{CCl}_4$  solution (Figure 11a for BN and Figure 12a for o'TN), we observe again that one band is located at higher and the other band at lower frequencies. However, in these samples the intensity ratio between the lower and the higher frequency bands is lower than for PN and IBN, but higher than for AN and PrN. Thus, although the hindering influence has been corroborated, additional factors should be involved.

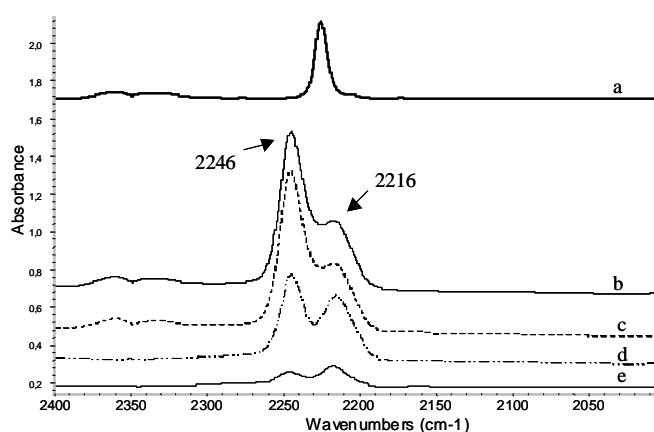


**Figure 12.** FT-IR spectra of liquid o'TN (a), in the presence of o'TN (b) and after evacuation at room (c) at 473 K (d) and 573 K (e).

Therefore, for all nitriles tested, a new band due to species more resistant to outgassing, whose CN stretching frequency is shifted to lower frequencies, is formed. This band is more intense for the more hindered nitriles (that do not access the cavities) than for smaller molecules. This indicates that the interaction takes place on the outer surface or on the mouth of the main channels. The interpretation that we can propose for these species is to

hypothesize a complex and probably multiple interaction of CN groups with  $\text{Na}^+$  cations or  $\text{Na}^+$  cations and framework oxygens.

Besides, the CN stretching band shifted downwards is more resistant to outgassing than the band shifted upwards for nitriles whose access even to the main channels is very highly hindered (PN, BN and oTN), whereas for the smaller molecules (AN, PrN and IBN) this band is relatively weaker. In order to explain the adsorption behaviour obtained for these nitriles, a comparative discussion is presented, for which aromatic nitriles have not been taken into account since the comparison becomes difficult due to their different nature. Table 2 shows the relation between peak areas obtained for aliphatic nitriles with respect to the acetonitrile one. Liquid phase nitrile spectra have been collected in diluted  $\text{CCl}_4$  solution using quantitative conditions. Peak areas obtained for adsorbed nitriles spectra have been normalized to the disk weight. The data show that the absolute intensity of the CN stretching modes (in the case of AN both components of the Fermi Resonance double have been considered) tends to increase in the order  $\text{AN} < \text{PrN} < \text{IBN} \approx \text{PN}$  in  $\text{CCl}_4$  solution (Table 2), while exactly the inverse tendency is found for nitriles adsorbed on NaMOR, where the amount of nitrile adsorbed follows the trend  $\text{AN} > \text{PrN} \gg \text{IBN} > \text{PN}$ . This can be easily understood considering that AN and PrN have free access to the main channels and side pockets, while for IBN and PN the access to the side pockets is likely forbidden. Taking into account the dimensions of the main channels ( $6.7 \text{ \AA} \times 7.0 \text{ \AA}$ ) and the ionic radius of the  $\text{Na}^+$  cations ( $0.95 \text{ \AA}$ ), as well as, the critical diameter of the isopropyl group ( $5 \text{ \AA}$ ) and tertbutyl group ( $6 \text{ \AA}$ ), i. e. alkyl groups of IBN and PN respectively, it is easy to conclude that the access of PN to the main channels is likely forbidden, but even that for IBN is probably highly hindered. Therefore, the spectrum observed for adsorbed AN is essentially the result of the sum of the spectra of AN in the side pockets, in the main channels and in the outer surface. In contrast, the spectra of adsorbed PN are only due to the interaction

occurring on the outer surface and on the channel mounths. The cases of PrN and IBN are somehow intermediate.

**Table 2.** Peak area relation for aliphatic nitriles respect to the AN one, in CCl<sub>4</sub> solution (L) and adsorbed on NaMOR (A).

	L (in solution)	A (adsorbed)	A/L
AN	1	1	1
PrN	1.14	0.90	0.79
IBN	1.65	0.45	0.27
PN	1.56	0.32	0.20

The adsorption of a hindered nitrile, PN, has been investigated also on a commercial Na-X zeolite and on a Silica-alumina highly impregnated with Na<sup>+</sup> cations for comparison,. The spectra of PN adsorbed on NaX zeolite are reported in Fig. 13a - 13c, where the CN stretching band of adsorbed PN is found, quite broad, after outgassing at room temperature at 2240 cm<sup>-1</sup>. By outgassing at progressively higher temperatures, the intensity band decreases and the main maximum shifts to higher frequency up to 2250 cm<sup>-1</sup>, showing some heterogeneity of the adsorption sites. The maximum rises to a similar position (but a little shifted downwards) that found for Na-MOR. However, also in this case upon outgassing at 473 K a component appears at lower frequency, namely at 2223 cm<sup>-1</sup>, near the same position as observed for Na-MOR in the same conditions.

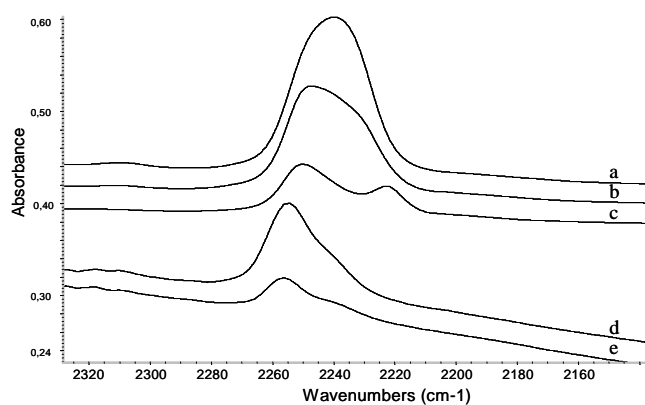


**Figure 13.** FT-IR of adsorbed PN on NaX evacuated at room temperature (a), at 373 K (b) and 473 K (c), and on NaSilicaAlumina evacuated at room temperature (d), and at 373 K (e).

In the case of PN adsorption on Na-Silica-alumina (Figure 13d–13e), the main band is again observed well shifted upwards, at even higher frequencies (2257 cm<sup>-1</sup>), with a shoulder centered near 2238 cm<sup>-1</sup>, but in this case, the lower frequency component does not appear. This supports the idea that the complex interaction responsible for the lower frequency band occurs at the mouths of the channels.

#### **5.1.3.7. Coadsorption AN + CO**

The co-adsorption of AN and CO has been performed as described on the experimental section. The obtained spectra are shown in Figure 14.

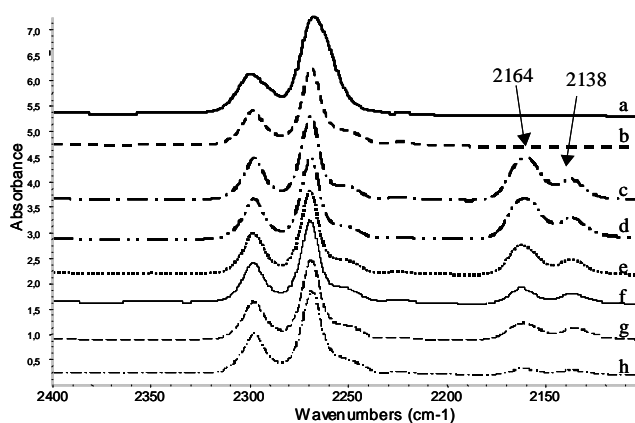


**Figure 14.** FT-IR of adsorbed AN on NaMOR at room temperature (a) evacuated at 373 K and cooled at 133 K (b) after CO adsorption at 133K (c), under evacuation at 143 K (d), 173 K (e), 193 K (f), 213 K (g), 233 K (h).

As we have previously described, the maxima of the bands of adsorbed AN on NaMOR slightly shift to higher frequencies upon outgassing at increasing temperatures. This shows the heterogeneity of the adsorption sites. After outgassing at 373 K the intensity of the band diminishes a factor of 0,3. This indicates that AN is desorbed from the weaker sites, while still interacts with the stronger ones, and by co-adsorbing CO in these conditions the spectra now show two bands at 2164  $\text{cm}^{-1}$  and 2138  $\text{cm}^{-1}$ . The shoulder at higher frequencies (2175  $\text{cm}^{-1}$ ), which is present when adsorbing only CO (Figure 4), is absent here. Therefore, CO is able to access the weakest sites, that have been freed by AN, while it cannot displace the AN adsorbed on the stronger sites. However, interestingly, the low frequency component at 2138  $\text{cm}^{-1}$  is already formed just after contact with CO.

#### ***5.1.4. Conclusions***

The data described and discussed above, may allow us to have deeper information on the NaMOR structure and its interaction with several adsorbates.

By comparing X-ray diffraction patterns and skeletal FIR spectra of NaMOR and HMOR, it is possible to conclude that Na<sup>+</sup> cations are randomly matched on the mordenite cavities.

Low temperature CO adsorption experiments show two different Na<sup>+</sup>····CO complexes characterized by different frequencies that are enhanced respect to the free molecule spectrum. These complexes can be assigned to single CO molecules interacting with single Na<sup>+</sup> cations in two different positions, main channels and side pockets. Parallel experiments performed on HMOR show quite clearly that CO first interacts with the Brönsted sites located on the main channels and later diffuses into those located in the side pockets. By outgassing, CO molecules first desorb from the sites located in the side pockets and later leave those of the main channels. This behaviour agrees with the stronger perturbation of the OHs located in the main channels showing in agreement with Maache et al. that the OHs in the main channels are likely more acidic, or in any case give a stronger interaction with CO, than those in the side pockets. Thus, in HMOR interaction with a so small molecule as CO, adsorption/desorption phenomena are mostly determined by adsorption strength more than by diffusion phenomena.

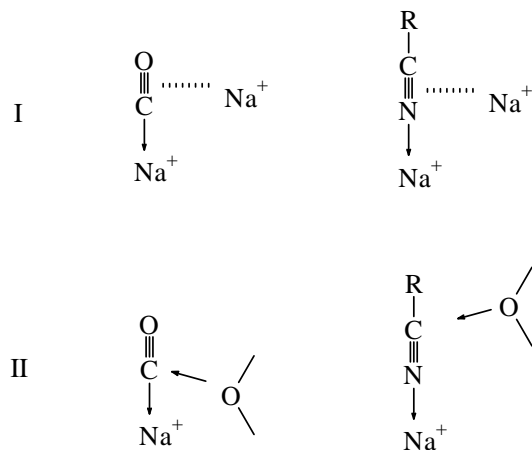
However, in the case of CO adsorption on NaMOR, a third, even stronger and perhaps activated, adsorption mode seems to occur. According to our results, the band observed at 2138 cm<sup>-1</sup>, and previously assigned at liquid-like CO, contains an additional component that resists outgassing at 233 K. This quite stable species should be assigned to CO molecules involved in a multiple

perturbation that causes a slight decrease on the CO stretching frequency. Being these species not observed on HMOR, it seems likely that this interaction involves  $\text{Na}^+$  cations.

Adsorption of nitriles characterized by differently hindered hydrocarbon entities, show in all cases the formation of complexes with  $\text{Na}^+$  cations. The adsorption of AN shows a clear heterogeneity of the adsorption sites and shows that, as expected, the species characterized by the stronger perturbation are more resistant when outgassing. Also, in this case, consequently, adsorption/desorption phenomena seem to be mostly determined by adsorption strength more than by diffusion phenomena. In the case of PN, which was previously found to access, very slowly, only to the main channels of HMOR, the access to the cavities of NaMOR is like fully forbidden. Thus is also very likely the case of BN and oTN. However, although such big hydrocarbon entities cannot enter the cavities, the CN can do this by interacting with the  $\text{Na}^+$  cations located either at the external surface or near the mouth of the channels.

For all nitriles, additionally to that band with a CN stretching frequency located at higher frequencies than the liquid value (CN shift 15-20  $\text{cm}^{-1}$ ), a new band is formed at frequencies near or slightly below than the liquid value, whose stability seems to be higher than the usual ones. The behaviour observed for all nitriles, at 300-500 K seems to parallel that observed for CO at 150-250 K. A new band associated to more resistant species is observed, with a CN stretching frequency shifted lower than the liquid value. The interpretation that we propose for these species is to hypothesize multiple interactions where CN groups interact with  $\text{Na}^+$  cations or  $\text{Na}^+$  cations and framework oxygen atoms (Scheme 1 for possible structures). The fact that this interaction is more important for highly hindered molecules together with that it does not appear

on Na-Silica-alumina, where zeolitic pores do not exist, suggests that the interaction takes place on the mouth of the main channels.



**Scheme 1.** Tentative structures for the strongest interactions of CO and nitriles on NaMOR. I: interactions with two  $\text{Na}^+$  ions. II: Interaction with  $\text{Na}^+$  and  $\text{O}^=$  ions.

### 5.1.5. References

- <sup>1</sup> Guisnet, M.; Gilson, J.P., eds., *Zeolites for cleaner technologies*, Imperial College Press: London, Catalytic Science Series, Vol 3, 2002, p. 209.
- <sup>2</sup> van Bokhoven, J.A.; Tromp, M.; Koningsberger, D.C.; Miller, J.T.; Pieterse, J.A.Z.; Lercher, J.A.; Williams, B.A.; Kung, H.H. *J. Catal.* **2001**, 202, 129.
- <sup>3</sup> Moreau, F.; Ayrault, P.; Gnep, N. S.; Lacombe, S.; Merlen, E.; Guisnet, M. *Micropor. Mesopor. Mat.* **2002**, 51, 211.

- <sup>4</sup> Weitkamp, J.; Hunger, M.; Rymasa, U. *Micropor. Mesopor. Mat.* **2001**, 48, 255.
- <sup>5</sup> Davis, R. J. *J. Catal.* **2003**, 216, 396.
- <sup>6</sup> Martra, G.; Ocule, R.; Marchese, L.; Centi, G.; Coluccia, S. *Catal. Today* **2002**, 73, 83.
- <sup>7</sup> Armaroli, T.; Finocchio, E.; Busca, G.; Rossini, S. *Vib. Spectrosc.* **1999**, 20, 85.
- <sup>8</sup> Pamba, M.; Maurin, G.; Devautour, S.; Vandershueren, J.; Giuntini, J. C.; Di Renzo, F.; Hamidi, F. *Phys. Chem. Chem. Phys.* **2000**, 113, 4498.
- <sup>9</sup> Devautour, S.; Abdoulaye, A.; Giuntini, J.C.; Henn, F. *J. Phys. Chem. B* **2001**, 105, 9297.
- <sup>10</sup> Bell, R. G.; Devautour, S.; Henn, F.; Giuntini, J. C. *J. Phys. Chem. B* **2004**, 108, 3739.
- <sup>11</sup> Webster, C. E.; Cottone, A.; Drago, R.S.; *J. Am. Chem. Soc.* **1999**, 121, 12127.
- <sup>12</sup> Yuvaray, S.; Chang, T. H.; Yeh, C. T. *J. Phys. Chem. B* **2003**, 107, 4971.
- <sup>13</sup> Salla, I.; Salagre, P.; Cesteros, Y.; Medina, F.; Sueiras, J. E. *J. Phys. Chem. B* **2004**, 108, 5359.
- <sup>14</sup> Knözinger, H.; Huber, S. J. *Chem. Soc., Faraday Trans.* **1998**, 94 (15), 2047.
- <sup>15</sup> Hadjiivanov, K. I.; Vayssilov, G. N. Characterization of oxide surfaces and zeolites by Carbon Monoxide as an IR Probe Molecule in *Advances in Catalysis*, Academic Press, 2002, Vol 47, p 307.
- <sup>16</sup> Onida, B.; Monelli, B.; Borello, L.; Fiorilli, S.; Geobaldo, F.; Garrone, E. *J. Phys. Chem. B* **2002**, 106, 10518.
- <sup>17</sup> Marie, O.; Massiani, P.; Thibault-Starzyk, F. *J. Phys. Chem. B* **2004**, 108, 5073.
- <sup>18</sup> Bordiga, S.; Lamberti, C.; Geobaldo, F., Zecchina, A.; Turnes Palomino, G.; Otero Areán, C. *Langmuir* **1995**, 11, 527.

- <sup>19</sup> Bevilacqua M.; Gutiérrez-Alejandre A.; Resini C.; Casagrande M.; Ramírez J.; Busca G. *Phys. Chem. Chem. Phys.* **2002**, 4, 4575.
- <sup>20</sup> Bevilacqua, M.; Busca, G. *Catal. Commun.* **2002**, 3, 497.
- <sup>21</sup> Montanari, T.; Bevilacqua, M.; Resini, C.; Busca, G. *J. Phys. Chem. B* **2004**, 108, 2120.
- <sup>22</sup> Busca G.; Resini, C. Vibrational spectroscopy for the analysis of geological and inorganic materials, in *Encyclopedia of Analytical Chemistry*, R.A. Meyers eds., Wiley, Chichester, 2000, p. 10984.
- <sup>23</sup> Tsyganenko, A. A.; Escalona Platero, E.; Otero Areán, C.; Garrone, E.; Zecchina, A.; *Catal. Letters* **1999**, 61, 187.
- <sup>24</sup> Maache, M.; Janin, A.; Lavalley, J. C.; Benazzi, E. *Zeolites* **1995**, 15, 507.
- <sup>25</sup> Zecchina, A.; Geobaldo, F.; Spoto, G.; Bordiga, S.; Ricchiardi, G.; Buzzoni, R.; Petrini, G. *J. Phys. Chem.* **1996**, 100, 16584.
- <sup>26</sup> Angell, C. L.; Howell, M. V. *J. Phys. Chem.* **1969**, 73, 2551.
- <sup>27</sup> Armaroli, T.; Finocchio, E.; Busca, G. Rossini, S. *Vib. Spectrosc.* **1999**, 20, 85-94.
- <sup>28</sup> Reedijk, J.; Zuur, A.P.; Groeneveld, W.L. *Recueil* **1967**, 86, 1127.

## 5.2. A reexamination of the adsorption of CO and nitriles on alkali-metal-mordenites: characterization of multiple interactions\*

### *Abstract*

Low temperature CO adsorption and room temperature propionitrile and ortho-toluonitrile adsorption on LiMOR, NaMOR, KMOR and CsMOR zeolites have been investigated by FT-IR spectroscopy. Two different CO species, probably located in the main channels coordinated to Na<sup>+</sup> at IV and VI sites, have been observed. These are associated to a shift of the CO stretching to higher frequencies, as usual. However, together, more strongly bonded species associated to a slight shift of the CO stretching to lower frequency are also observed. Similar species, with the CN stretching shifted upwards (weaker adsorption) and with the CN stretching shifted downwards (stronger adsorption) are also observed in the case of the interaction of propionitrile and ortho-toluonitrile. The data show that the species characterized by a stronger adsorption but a lower stretching frequency may form both in the main channels and at the external surface. Their formation is easier with the larger cations. These species are identified as “multiply bonded” species. The evidence for this new interaction, stronger than the usual one site–one molecule species, may change considerably the view of the adsorption chemistry of cationic zeolites, from localized simple sites to cooperative complex interactions.

---

\* Physical Chemistry Chemical Physics **2005**, 7 (12), 2526-2533.

### ***5.2.1. Introduction***

Light alkali metal exchanged zeolites (like e.g. Na-A, Li-MOR, Na-X and Na-Y) act as selective regenerable adsorbants for purification of gaseous streams<sup>1</sup> or for the separation of industrial products (e.g. the xylenes separation<sup>2</sup> and the oxygen-nitrogen air separation<sup>3</sup> on alkali-metal X or Y) and as quite mild basic catalysts as well.<sup>4,5</sup> Whereas, heavy-alkali metal zeolites (like Cs-Y) are reported to be strong bases.

Mordenite is a medium pore zeolite, which finds, in its protonic (HMOR) or partially Na-exchanged (NaHMOR) forms, application in the industry for several hydrocarbon conversions.<sup>6-8</sup> Alkali-metal exchanged MOR have been the object of investigations in particular for their ability to adsorb nitrogen and for the possibility to substitute Na-FAU adsorbants used for the industrial separation of air's N<sub>2</sub> from O<sub>2</sub> in pressure swing adsorption processes.<sup>9-11</sup>

The orthorhombic mordenite structure<sup>12</sup> is characterized by nearly straight “main” channels running along the [001] crystallographic direction, which are accessible through twelve-membered (elliptical) silicon-oxygen rings having 6.5 Å x 7.0 Å diameters. Additionally, 8-ring “side pockets” exist in the [010] direction having 3.4 Å x 4.8 Å diameter, which however do not allow flow of molecules being in fact interrupted by narrow-necked obstructions. The side pockets connect the twelve ring main channel to a distorted eight-ring channel also running parallel to the [001] direction, but having an elliptical compressed opening 5.7 Å x 2.6 Å wide. The localization of Na<sup>+</sup> in Na-MOR samples has been the object of several studies.<sup>12-16</sup> Assuming the idealized composition for dehydrated MOR Na<sub>8</sub>Si<sub>40</sub>Al<sub>8</sub>O<sub>96</sub> (Si/Al = 5) it seems quite established that half of Na<sup>+</sup> ions are located just in the middle of the small compressed channels in the site called (I) or A. These Na ions do not move upon water adsorption and cannot bind adsorbed water. Location (I) or A is also fully occupied for MOR

samples with Si/Al = 11. It is usually supposed that only monoatomic species can enter the compressed channels of NaMOR and interact with cations in sites A. The other half Na<sup>+</sup> ions are distributed between site IV, also called D, near the opening of the side pocket in the main channel, and in position VI, also called E, which is well exposed in the main channel. The theoretical occupation degree of each site is 4,3,1 for A, D, E.<sup>14</sup>

The low temperature adsorption of CO is today perhaps the most popular technique for characterizing adsorption sites of zeolites in IR spectroscopy.<sup>17-20</sup> This technique has been applied to investigate the properties of alkali metal mordenite, showing the formation of two kinds of alkali ion carbonyl species associated to different cation locations either in the main channels or in the side pockets.<sup>21-23</sup> The polarizing effect of the cation was found to constitute the main factor influencing the CO stretching frequency although the polarity of the zeolite framework has also an effect.

In a more recent IR study on Na-MOR, the adsorption of different hindered nitriles together with CO were used for zeolitic sites characterization. Evidence has been provided for the formation of more complex interactions, where the adsorbate molecule interacts with more than one site, has been reported by us.<sup>24</sup> The formation of such species has later been shown also for nitriles adsorbed on NaX and NaY faujasites.<sup>25</sup>

To have more information on such new species and on the localization of the different adsorption sites, we re-investigated the alkali-metal zeolite systems by using both nitriles and CO as adsorption probes.

### ***5.2.2. Experimental***

Na-MOR (Si/Al = 6.5, CBV 10A Lot No. 1822-50) was supplied by Zeolyst as hydrated powder. The chemical composition was SiO<sub>2</sub>/Al<sub>2</sub>O<sub>3</sub> mole ratio 13 and a Na<sub>2</sub>O weight % of 6.6. H-MOR was prepared by cation exchanging the starting form, Na-MOR, with a NH<sub>4</sub>Cl 2.2 M solution and later calcining at 673 K. LiMOR, KMOR and CsMOR samples were obtained by cation exchanging three times the NaMOR zeolite with the corresponding chloride salt 2.2 M.

Powder X-ray diffraction patterns of the samples were obtained with a Siemens D5000 diffractometer (Bragg-Brentano parafocusing geometry and vertical  $\theta$ - $\theta$  goniometer) fitted with a curved graphite diffracted-beam monochromator, incident and diffracted-beam Soller slits, a 0.006° receiving slit and scintillation counter as a detector. The angular  $2\theta$  diffraction range was between 5° to 70°. The data were collected with an angular step of 0.05° at 3s per step and sample rotation. CuK $\alpha$  (1.542 Å) radiation was obtained from a copper X-ray tube operated at 40kV and 30mA. The cell parameters and cell volume values were calculated using a matching profile with TOPAS 2.0 software (Bruker AXS).

Skeletal MIR (KBr pressed disks) and FIR (pure powder on polyethylene supports) spectra were recorded on a Nicolet Magna 750 Fourier Transform instrument (resolution 4 cm<sup>-1</sup>). Additionally, both samples were characterized (on MIR range) by adsorbing several probe molecules. Different nitriles like propionitrile (PrN) and o-toluenitrile (o-TN) were used to characterize mordenite samples, and furthermore CO at low temperature was also used. The pressed disks of pure zeolite powders were activated “in situ” the IR cell by outgassing at 773 K before the adsorption experiments. A conventional gas manipulation/outgassing ramp connected to the IR cell was used. The adsorption/desorption process has been studied by transmission FT-IR. For nitriles, the adsorption procedure involves contact of the activated sample disk

with vapors at room temperature at a pressure not higher than 2.5 kPa. The desorption process at increasing temperatures was performed in vacuum at temperatures in the range between 273K and 573K. On the other hand, CO adsorption was performed a 130 K by the introduction of a well-known dose of the gas inside the low temperature infrared cell containing the previously activated wafers. IR spectra were collected evacuating at increasing temperatures between 130 and 273 K.

### ***5.2.3. Results.***

#### ***5.2.3.1. Skeletal MIR and FIR spectra***

Figure 1 shows the X-ray Diffraction patterns obtained for the alkali- cation MOR samples. They agree to their respective Mordenite JCPDS files. The samples present similar cristallinity, and no significant differences on the peak width are appreciable from X-ray patterns. Only in the case of CsMOR, the peaks intensities are a bit different, in agreement with the data reported in the corresponding JCPDS file (01-083-1627 for CsMOR). No structural changes can be observed in all cases from the corresponding JCPDS file fit. Thus, these intensity changes are likely due to the effect of electronic parameters of Cs that are quite different from those of other cations. The calculated cell parameters and cell volume for all samples are also reported in Table 1. The variation of cell volume values observed could be related to the real hydrated cation size. The absence of hkl peaks associated to a cation match on structure, suggests that cations may be randomly distributed on our samples.

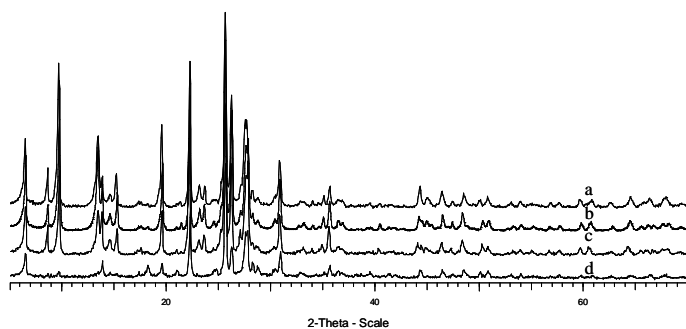


**Figure 1.** X-ray Diffraction patterns of LiMOR (a), NaMOR (b), KMOR (c) and CsMOR (d) samples.

**Table 1.** Cell parameters of HMOR and alkali-MOR samples calculated by XRD.

	a (Å)	b (Å)	c (Å)	cell vol. (Å <sup>3</sup> )
HMOR	18.0979(41)	20.4470(31)	7.5109(10)	2779
LiMOR	18.1985(30)	20.4095(25)	7.4907(8)	2782
NaMOR	18.1063(16)	20.4533(13)	7.5143(4)	2783
KMOR	18.1142(37)	20.5163(28)	7.5159(8)	2793
CsMOR	18.2036(40)	20.4157(41)	7.4955(13)	2786

In Figure 2, the skeletal MIR/FIR spectra (KBr and polyethylene pressed disks, respectively) for HMOR and alkali metal MOR samples are reported. The spectra compare well with those reported in the literature<sup>26</sup>. Slight shifts (few cm<sup>-1</sup>) of the main maxima are found, showing a slight effect of the hydrated cations on the vibrations of the framework.

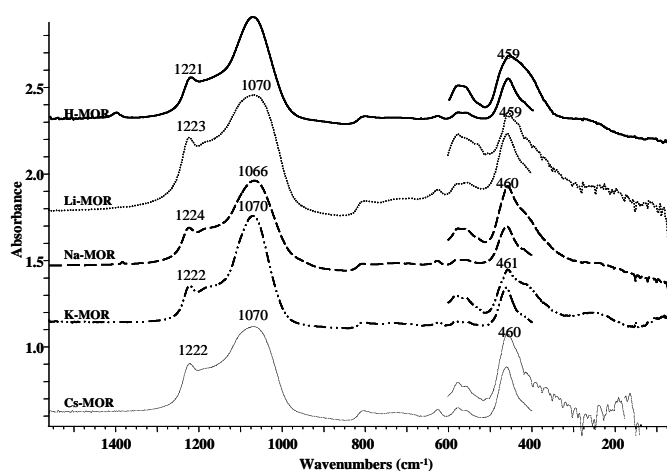


**Figure 2.** Skeletal MIR (1500-400  $\text{cm}^{-1}$ ) and FIR (600-50  $\text{cm}^{-1}$ ) of HMOR, LiMOR, NaMOR, KMOR and CsMOR.

The spectra of pressed disks of the pure MOR powders after activation in vacuum show in the region 2100-1600  $\text{cm}^{-1}$  broad absorptions due to harmonics of the fundamental skeletal modes, as usually observed. These features are relevantly shifted down the more the heavier the cations, more than expected by looking at the corresponding fundamentals. The two main maxima are observed at 1636, 1862  $\text{cm}^{-1}$  for LiMOR, 1626, 1860  $\text{cm}^{-1}$  for NaMOR, at 1620, 1839  $\text{cm}^{-1}$  for KMOR and at 1614, 1838  $\text{cm}^{-1}$  for CsMOR. This suggests a stronger effect of the naked extraframework ions with respect to the hydrated ones on the mechanics of the framework.

### 5.2.3.2. Spectra of the surface hydroxy groups

The overall spectrum of activated alkali metal -MOR samples (pure powder pressed disks) in the 4000-3200  $\text{cm}^{-1}$  range are compared to the spectrum of HMOR sample in Figure 3. In the OH stretching region for HMOR sample, two bands can be observed: the first at 3744  $\text{cm}^{-1}$  associated to the terminal

silanol groups, and the second one (very strong and complex) with the main maximum at  $3605\text{ cm}^{-1}$ , assigned to the bridging Si-OH-Al groups. According to Bevilacqua et al. such OH groups are exclusively located on the inner surface and possess a strong Brønsted acidity.<sup>27,28</sup> The asymmetry of this band indicates the presence of different components. At least three components were previously identified by Bevilacqua et al.<sup>26,27</sup> and later confirmed by Marie et al.<sup>23</sup> An additional weak component can be observed for HMOR sample at  $3655\text{ cm}^{-1}$ , which can be associated to small amounts of extraframework aluminum species formed during the activation by heating in vacuo.

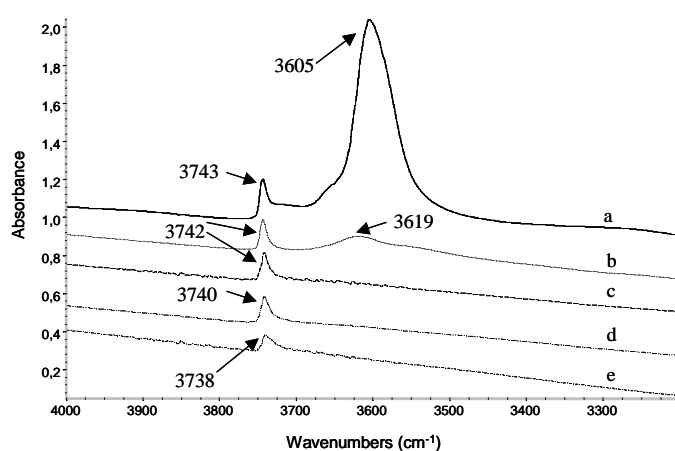


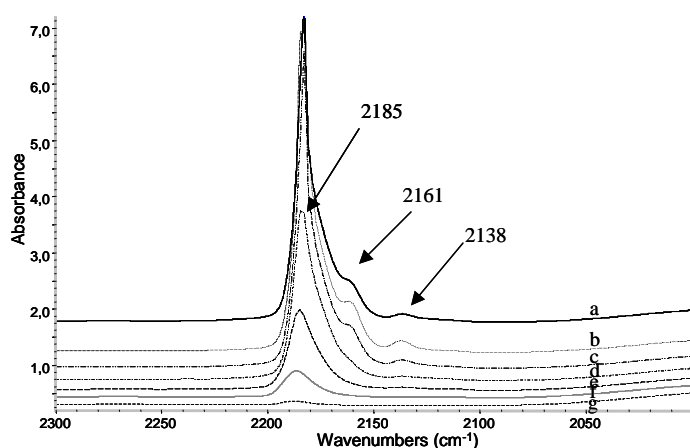
**Figure 3.** FT-IR spectra on the OHs region of HMOR (a), LiMOR (b), NaMOR (c), KMOR (d) and CsMOR (e) samples activated at 773 K in vacuum conditions.

In the case of Na-, K- and CsMOR the absence of the band centered at  $3605\text{ cm}^{-1}$  indicates that all the possible internal positions are occupied by alkali cations. Only in the case of Li-MOR some absorption is present near  $3610\text{ cm}^{-1}$ , as observed for a similar sample also by Geobaldo et al.,<sup>29</sup> who assigned this band to unexchanged proton sites. Thus, in our case these protonic sites could have been generated during NaMOR exchange with LiCl solution.

In all cases, a sharp band is present above 3700  $\text{cm}^{-1}$ , suggesting that external silanols are present and not exchanged. In the case of LiMOR and NaMOR this band is just at 3744-5  $\text{cm}^{-1}$ , so really unshifted with respect to H-MOR and all typical “unperturbed” silanol groups. However, in the case of KMOR and CsMOR this band is found at a lower frequency, down to 3738  $\text{cm}^{-1}$ . This effect, not reported previously,<sup>29</sup> may be related to the overall effect of the exchanging cations on the mechanics of the framework, as shown above for skeletal vibrations, or to effect of some alkali cations outside the channels on the external surface where terminal silanols are located.

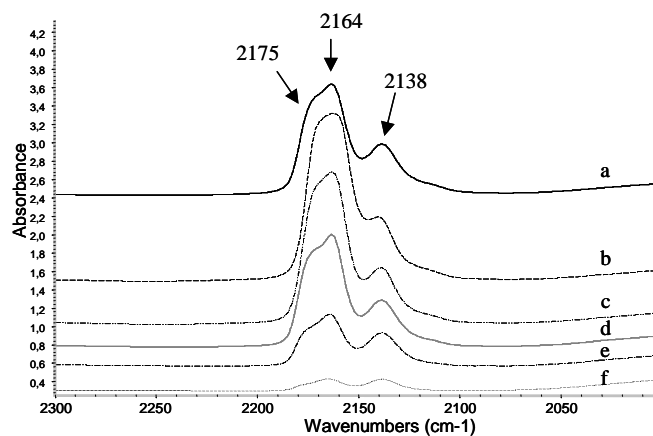
### ***5.2.3.3. Low temperature adsorption of CO on Li-, Na-, K- and Cs-MOR***

Figure 4 shows the IR bands of adsorbed CO on LiMOR under evacuation at low temperature. At 133 K, a single sharp band is observed in the CO stretching range, with two weaker components at lower frequency. The first one, intense, quite narrow and asymmetric, with a tail towards lower frequencies shows the main maximum at 2185  $\text{cm}^{-1}$ , the second band is centered at 2161  $\text{cm}^{-1}$ , and the last band has a maximum centered at 2138  $\text{cm}^{-1}$ . By progressively increasing temperature upon outgassing, the higher frequency band progressively decreases its intensity. In the same way, the bands at 2161  $\text{cm}^{-1}$  and 2138  $\text{cm}^{-1}$  also decrease in intensity, but they do it much faster up to their complete disappearance during evacuation at 193 K.



**Figure 4.** FT-IR spectra of LiMOR in the presence of CO under evacuation at 133 K (a), at 143 K (b), 173 K (c), 193 K (d), 203 K (e), 233 K (f) and 263 K on the CO stretching range.

In the case of CO adsorbed on NaMOR (Figure 5) two main bands were observed on the CO stretching range with the main maximum at  $2164\text{ cm}^{-1}$  and a shoulder at  $2175\text{ cm}^{-1}$  and the second band, less intense, located at  $2138\text{ cm}^{-1}$ . By progressively increasing temperature upon outgassing, the higher frequency band together with its shoulder parallelly decrease their intensity. In the same way, the lower frequency band decreases in intensity, but much slower, when temperature increases. This band, which is initially weaker than the higher frequency band, has finally a similar intensity at 113 K and 233 K.



**Figure 5.** FT-IR spectra of NaMOR in the presence of CO gas at 133 K (a), and under evacuation at 143 K (b), 173 K (c), 193 K (d), 213 K (e), 233 K (f) on the CO stretching range.

The IR bands of adsorbed CO on KMOR under evacuation are shown in Figure 6. At 133 K at least four components are observed on the CO stretching, with the main maximum at  $2161\text{ cm}^{-1}$  and shoulders of decreasing intensities at  $2150\text{ cm}^{-1}$ ,  $2134\text{ cm}^{-1}$  and  $2117\text{ cm}^{-1}$ . By progressively increasing temperature upon outgassing, the two components at higher frequencies together with the band at  $2117\text{ cm}^{-1}$  parallelly decrease their intensity. Otherwise the band at  $2134\text{ cm}^{-1}$ , which also decreases its intensity under evacuation at increasing temperatures, does it much slower up to the point that at 223 K this band has higher intensity than the two bands at higher frequencies.

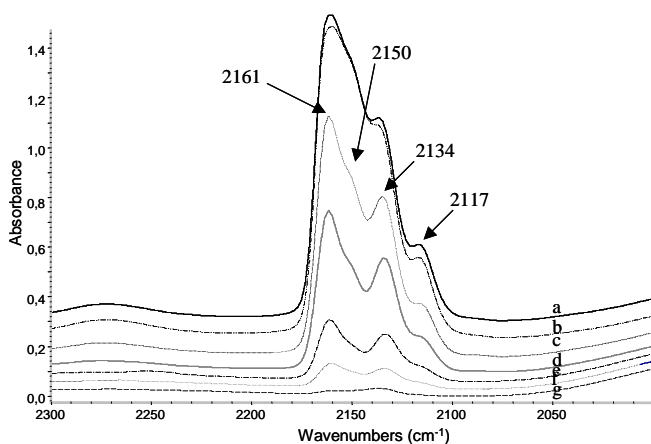


**Figure 6.** FT-IR spectra of KMOR in the presence of CO under evacuation at 133 K (a), at 153 K (b), 173 K (c), 183 K (d), 193 K (e), 203 K (f) and 223 K (g) on the CO stretching range.

Finally, for CsMOR, the IR bands of adsorbed CO under evacuation at different temperatures are shown in Figure 7. In all spectra three bands are observed on the CO stretching range at 2155  $\text{cm}^{-1}$ , 2143  $\text{cm}^{-1}$  and 2120  $\text{cm}^{-1}$ . The band at 2143  $\text{cm}^{-1}$  is the strongest in all spectra.

In the OH vibration range (not shown here), in all cases, the silanol band at around 3738-45  $\text{cm}^{-1}$  is not perturbed when mordenite samples are contacted with CO molecules, indicating that terminal silanol groups do not interact significantly with CO molecules in these conditions.

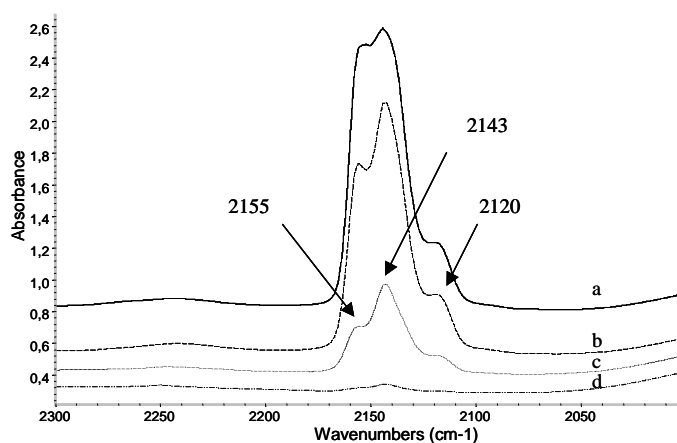


**Figure 7.** FT-IR spectra of CsMOR in the presence of CO under evacuation at 133 K (a), at 143 K (b), 153 K (c), 163 K (d), 173 K (e), 183 K (f) and 193 K (g) on the CO stretching range.

In all cases except LiMOR, a band at frequency lower or near that of “unperturbed” CO is observed, but is more resistant to outgassing than the higher frequency band. This behavior was examined by us previously in the case of NaMOR and this analysis, also supported by parallel experiments performed by using nitriles as adsorption probes, allowed us to reassign this band, previously attributed to liquid like CO,<sup>22,23</sup> to multiply bonded CO.<sup>24</sup> Only a multiple adsorption in fact can explain a stronger interaction with a lower CO stretching frequency. This assignment seems to be confirmed here. The bands observed at 2138 cm<sup>-1</sup> on NaMOR, at 2134 cm<sup>-1</sup> on KMOR and at 2143 cm<sup>-1</sup> on CsMOR show this behavior and may consequently be assigned to “multiply bonded” species in all cases. However, in the case of LiMOR a similar species is not observed, since the band at 2138 cm<sup>-1</sup> is attributed to physisorbed pseudo-liquid CO, because of its fast intensity decrease with increasing temperature.

In all spectra a weak band is also observed near 2120-2115  $\text{cm}^{-1}$ , for which a likely assignment is to O-bonded carbonyl species, as discussed elsewhere previously.<sup>29,30</sup>

#### ***5.2.3.4. IR study of the adsorption of propionitrile on Li-, Na-, K- and Cs- MOR***

Propionitrile (PrN) adsorption has been previously used to characterize the different cationic positions on H-MOR and Na-MOR, since it can access to all sites located in the main channels and side pockets.<sup>24,26,27</sup> As for the other nitrile molecules, the interaction of the N lone pair with electronwithdrawing centers causes a strengthening of the CN triple bond and a consequent shift upwards of the CN stretching frequency (2249  $\text{cm}^{-1}$  in the liquid<sup>32</sup>). This has been shown e.g. as in the case of nitrile metal complexes where metal cations act as Lewis acid sites,<sup>33</sup> as well as on Co-containing zeolites including Co-MOR<sup>34</sup> and in the case of the H-bonding complex with phenol<sup>35</sup> and meta-cresol<sup>36</sup> or on the acidic OHs of protonic zeolites.<sup>34</sup>

The spectra of PrN adsorbed on the different mordenite samples, and after outgassing at different temperatures are shown in Figures 8 to 11. The activated sample spectrum as well as the gas phase spectrum have been subtracted to all spectra. The same procedure has been applied to all adsorption experiments reported in this work. The nitrile spectrum on  $\text{CCl}_4$  solution, used as a reference, is also shown.

The subtracted spectra of PrN on LiMOR sample after outgassing at different temperatures are shown in Figure 8. At low temperatures (Figure 8b-c) we can observe a single but asymmetric CN stretching band shifted well above the position observed for the liquid (Figure 8a), whose maximum shifts from 2274 to 2278  $\text{cm}^{-1}$  by increasing outgassing temperature. However in the spectrum

collected after evacuation at 573 K (Figure 8e) a low intensity band appears at almost the same frequency than that of the liquid propionitrile (2249  $\text{cm}^{-1}$ ).

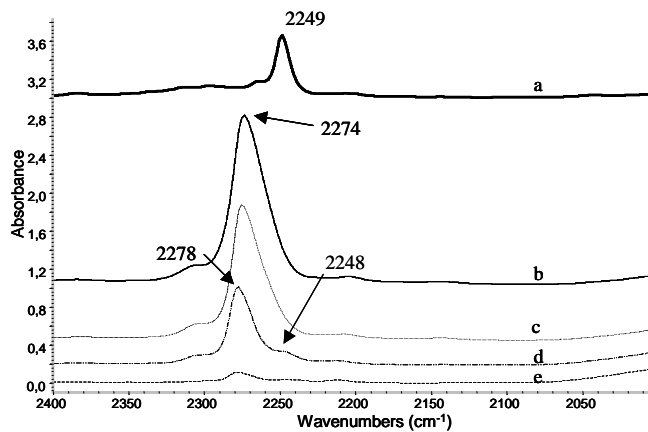


**Figure 8.** FT-IR spectra of liquid PrN (a), LiMOR in the presence of PrN after evacuation at room temperature (b) at 373 K (c), 473 K (d) and 573 K (e).

In the case of PrN adsorbed on NaMOR and after outgassing at different temperatures (Figure 9) an asymmetric band with a maximum at 2267  $\text{cm}^{-1}$  can be observed on the CN stretching region. The tail observed towards lower frequencies starts to disappear upon evacuation at room temperature (Figure 9b-9c). By increasing the temperature, the band intensity decreases and a new component at 2241  $\text{cm}^{-1}$  appears at 373 K. In that case this band is shifted well below the band of the liquid nitrile.

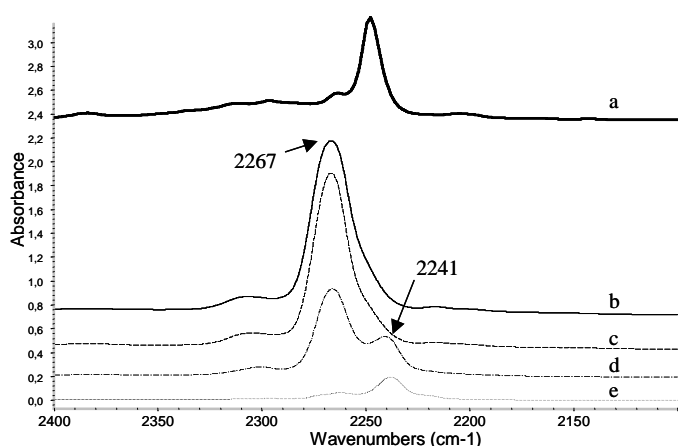


**Figure 9.** FT-IR spectra of PrN in CCl<sub>4</sub> solution (a), NaMOR in the presence of PrN vapors (b) and after evacuation at room temperature (c), 373 K (d) and 473 K (e).

The spectra of PrN adsorbed on KMOR are shown in Figure 10. In that case, the main band of adsorbed nitrile is centered at slightly lower frequency than that of the liquid nitrile. The position of this band is exactly at 2245 cm<sup>-1</sup> but a well resolved shoulder is evident at higher frequencies (around 2258 cm<sup>-1</sup>). In the spectrum collected after the evacuation at 473 K, the maximum of this band is shifted to lower frequencies down to 2241 cm<sup>-1</sup>, while the shoulder is still much weaker.

Also in the case of propionitrile adsorption on CsMOR (Figure 11), one band at slightly lower frequencies than the liquid nitrile is observed (2246 cm<sup>-1</sup>), which shifts to lower frequencies (down to 2242 cm<sup>-1</sup>) during evacuation at increasing temperatures.

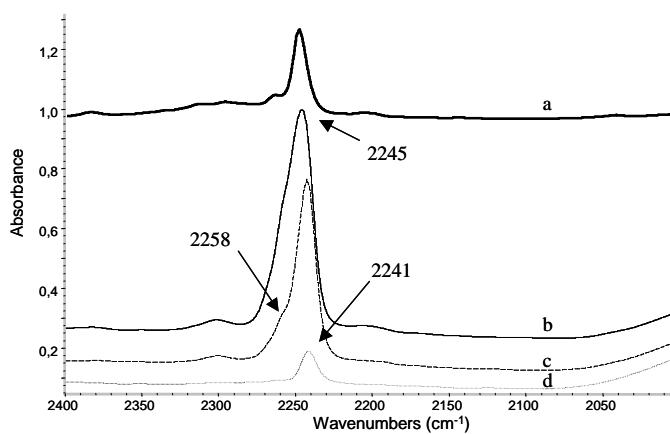


**Figure 10.** FT-IR spectra of liquid PrN (a), KMOR in the presence of PrN after evacuation at room temperature (b) at 373 K (c) and 473 K (d).

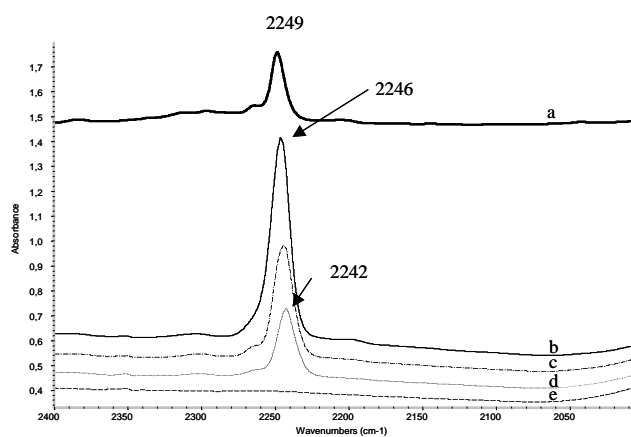


**Figure 11.** FT-IR spectra of liquid PrN (a), CsMOR in the presence of PrN after evacuation at room temperature (b) at 373 K (c), 473 K (d) and 573 K (e).

The formation of PrN adsorbed species characterized by a shift upwards of the CN stretching, as usual for molecules interacting with Lewis sites, is evident at least in the case of LiMOR (2274-2278 cm<sup>-1</sup>), NaMOR (2267 cm<sup>-1</sup>) and KMOR (2258 cm<sup>-1</sup>). As expected and in parallel with what has been shown for adsorbed CO, the position of this band shifts upwards the more the smaller the cation size, confirming that these features are associated to N-bonded species on cationic sites. In all cases, however, a strongly adsorbed species characterized by the CN stretching at quite low frequency (2250-2240 cm<sup>-1</sup>) is observed. This species has been previously identified by us, on NaMOR, as a “multiply bonded” species. The two bands are not resolved in the case of CsMOR at 2246 cm<sup>-1</sup>.

In all cases, a sharp band is present above 3700 cm<sup>-1</sup>, suggesting that external silanols are present and not exchanged. In the case of LiMOR and NaMOR this band is just at 3744-5 cm<sup>-1</sup>, so really unshifted with respect to H-MOR and all typical “unperturbed” silanol groups. However, in the case of KMOR and CsMOR this band is found at a lower frequency, down to 3738 cm<sup>-1</sup>. This effect, not reported previously,<sup>29</sup> may be related to the overall effect of the exchanging cations on the mechanics of the framework, as shown above for skeletal vibrations, or to effect of some alkali cations outside the channels on the external surface where terminal silanols are located.

#### ***5.2.3.5. IR study of the adsorption of orthotoluonitrile on Li-, Na-, K- and Cs- MOR***

Orthotoluonitrile (oTN) adsorption has been used to characterize basically the external positions of several zeolites including H-MOR and Co-MOR,<sup>34</sup> since its access to medium- and small-pore zeolite channels is highly hindered. Like other aromatic nitriles, such as benzonitrile, ortho-toluonitrile produces complexes through the coordination of its N lone pair to metal cations in metal

complexes<sup>37</sup> and on the surface of metal oxides.<sup>38</sup> Its CN stretching band, observed at 2225 cm<sup>-1</sup> in the case of the liquid<sup>39</sup> shifts upwards upon these interactions.

The spectra of oTN adsorbed on all the alkali-mordenite samples, and after outgassing at different temperatures are shown in Figures 12 to 15. Also in this case, the activated sample spectrum as well as the gas phase spectrum have been subtracted to the sample spectra. Ortho-toluonitrile spectrum in CCl<sub>4</sub> solution, used as a reference, is also shown.

Subtraction spectra of ortho-toluonitrile (oTN) adsorbed on LiMOR and after evacuation at increasing temperatures are shown in Figure 12. The CN stretching region shows two peaks, whose main maxima are centred at 2253 cm<sup>-1</sup> and 2217 cm<sup>-1</sup>. The frequency of the first band is higher than the frequency observed on the liquid nitrile spectrum (Figure 12a), as usual for species interacting with Lewis acid sites, whereas the second band is, unusually, at lower frequency than that of the liquid spectrum. At room temperature, the ratio between the peak area relating to “usual adsorbed species” and the peak area relating to “unusual low-frequency adsorbed species” decreases when temperature increases, showing that the “unusual low-frequency adsorbed species” is more strongly bonded.

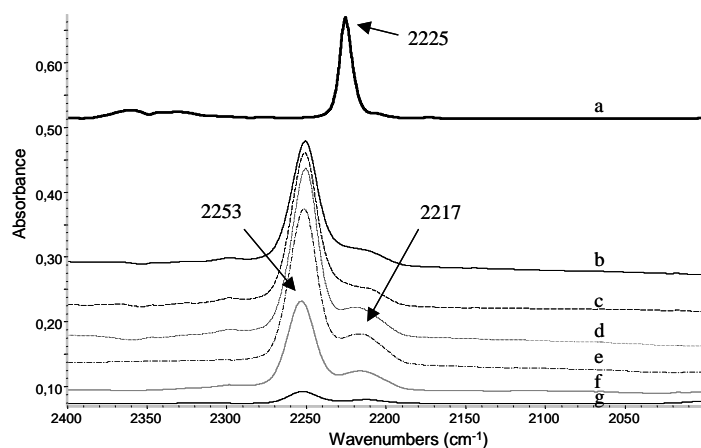


**Figure 12.** FT-IR spectra of liquid oTN (a), LiMOR in the presence of oTN (b) and after evacuation at room temperature (c) at 473 K (d), 573 K (e), 673 K (f) and 773 K (g).

The spectra of oTN on NaMOR show in the CN stretching region two peaks (Figure 13), whose main maxima are centred at 2246 and 2216  $\text{cm}^{-1}$ . The band at higher frequency is more intense than that at lower frequency, but during the desorption process, the intensity of the first one decreases faster, until they have similar intensity. Comparing those frequencies with that of the nitrile spectrum in  $\text{CCl}_4$  solution (Figure 13a) we observe again that one band is located at higher and the other band at lower frequencies.

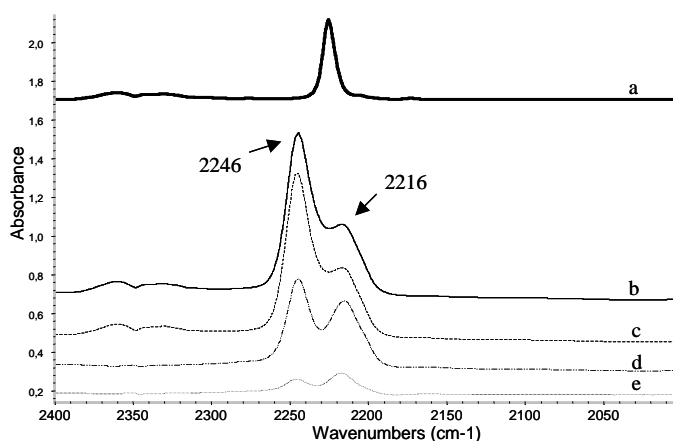


**Figure 13.** FT-IR spectra of liquid o'TN (a), in the presence of o'TN (b) and after evacuation at room (c) at 473 K (d) and 573 K (e).

In the case of KMOR (Figure 14), subtracted spectra of o'TN adsorbed on this sample and after evacuation at increasing temperatures show, in the CN stretching region, two peaks, whose maxima are centred at 2238  $\text{cm}^{-1}$  and 2224  $\text{cm}^{-1}$ . As it was observed for LiMOR and NaMOR samples, the frequency of the first band is higher than the frequency observed for the liquid nitrile, whereas the second band is at slightly lower frequency than that of the liquid nitrile spectrum. While on the spectra taken at lower temperatures (Figure 14b-d) the higher frequency band is more intense, at temperatures higher than 573 K (Figure 14e-g) the situation is completely reversed: the band at lower frequency is more intense than that at higher frequencies, and at desorption temperatures of 673 K and 773 K, only the band at 2224  $\text{cm}^{-1}$  is observed.

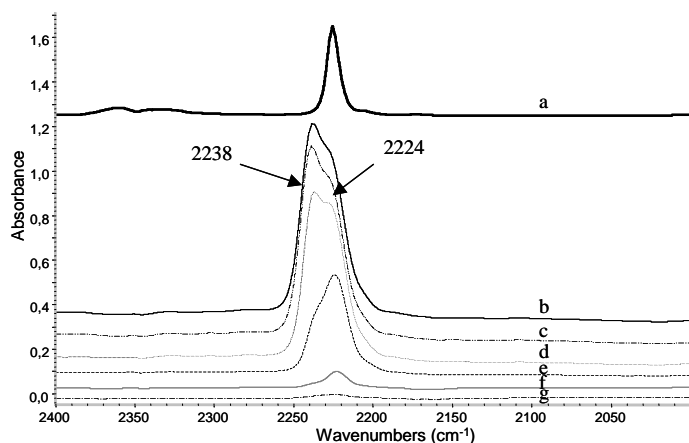


**Figure 14.** FT-IR spectra of liquid oTN (a), KMOR in the presence of oTN (b) and after evacuation at room temperature (c) at 473 K (d), at 573 K (e), at 673 K (f) and at 773 K (g).

Subtracted spectra of oTN adsorbed on CsMOR and after evacuation at increasing temperatures are shown in Figure 15. The spectra show in the CN stretching region one asymmetric band with the maximum at 2233  $\text{cm}^{-1}$  and a tail to lower frequencies. The band intensity decreases by increasing temperature and the main maximum shifts to lower frequencies until at 773 K the maximum is centered at 2227  $\text{cm}^{-1}$ .

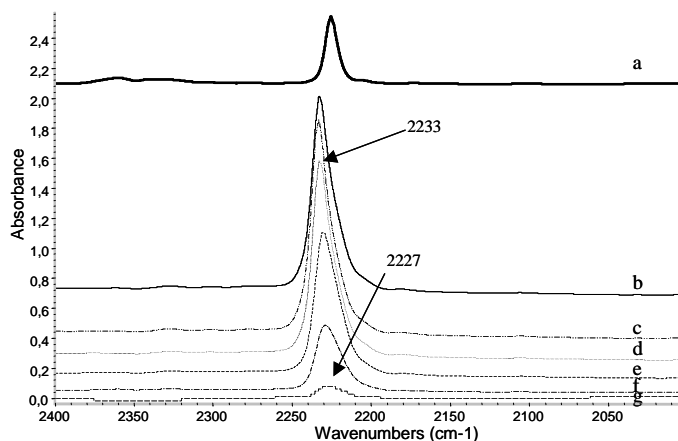


**Figure 15.** FT-IR spectra of liquid o'TN (a), CsMOR in the presence of o'TN (b) and after evacuation at room temperature (c) at 473 K (d), at 573 K (e), at 673 K (f) and at 773 K (g).

The higher frequency CN stretching component is found in all cases well above the liquid phase value while decreasing in the order LiMOR ( $2253\text{ cm}^{-1}$ ) > NaMOR ( $2246\text{ cm}^{-1}$ ) > KMOR ( $2238\text{ cm}^{-1}$ ) > CsMOR ( $2233\text{ cm}^{-1}$ ), in parallel with the decreasing acidity of the cations as already observed for adsorbed CO and PrN. This species may be identified as a “usual” species coordinated through the N lone pair to the different cations. However, due to the large size of o'TN, this interaction should occur out of the porous structure of mordenite or just at the mouth of the main channels.

Like in the case of PrN adsorption on alkali mordenites, the lower frequency component is also observed at least for LiMOR, NaMOR and KMOR and the CN stretching seems to follow the inverse trend: LiMOR ( $2217\text{ cm}^{-1}$ )  $\approx$  NaMOR ( $2216\text{ cm}^{-1}$ ) < KMOR ( $2224\text{ cm}^{-1}$ ). In the case of CsMOR the two bands nearly coincide. These results well indicate that this interaction should also occur just at the mouth of the main channels or, alternatively, on the external zeolite surface. It has, anyway to be taken into account that such an

interaction was not observed with a non-zeolitic material such as Na-silica alumina.<sup>24</sup>

#### **5.2.4. Discussion**

The data summarized above allow to improve the knowledge on the adsorption mechanisms occurring in the case of adsorption of gases and vapours on cationic zeolites. The data concerning CO adsorption on alkali mordenites fully agree with those reported previously.<sup>21-23</sup> In all cases it is evident the formation of C-bonded CO species whose stretching frequency shift increases by increasing the acidity of the cation, i.e. by decreasing its ionic radius. In the case of Na-MOR and K-MOR a splitting of this band is also quite evident, likely associated to two different accessible locations for Na<sup>+</sup> and K<sup>+</sup> cations. According to previous studies, in fact, Na<sup>+</sup> ions in NaMOR occupy three different sites. The most populated one, called (I) or A, is just in the middle of the compressed channels and is considered to be not accessible. The others are site IV, also called D, near the opening of the side pocket in the main channel, and site VI, also called E, which is well exposed in the main channel. In the case of CsMOR the same sites are likely occupied by Cs<sup>+</sup> ions.<sup>40,29</sup> Actually, as also shown in the computer simulations of Geobaldo et al. concerning N<sub>2</sub> adsorption on NaMOR the molecules adsorbed to the two accessible cations, at sites IV and VI, lay well in the center of the main channel, no adsorbed molecules being actually located in the side pockets. This makes less evident the reasons for the assignments given previously of the two components of the high frequency band.<sup>23</sup> Actually, the cations in position IV (near the center of an eight oxygen ring) appear to be more shielded by oxygens than those at position VI (off center of a six ring), and this allows us to assign the higher

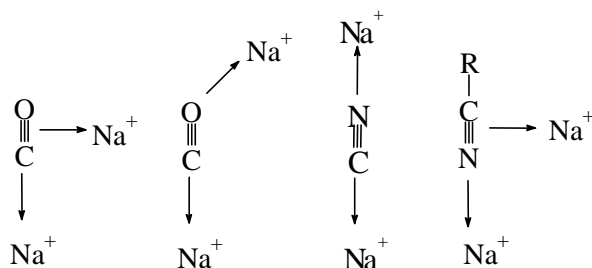
frequency component to CO C-bonded at position VI cations, the lower frequency one being assigned to CO C-bonded at position IV cations.

Similar species are also observed for propionitrile. N-bonded propionitrile molecules are well evident and, at least in the case of PrN adsorbed on LiMOR, the multiplicity of the CN stretching band, whose maximum shifts significantly upwards by decreasing coverage, may be an indication of the duplicity of the adsorbing ions (site VI and IV). This shift is less or not at all evident, in the case of PrN adsorbed on the other alkali-MOR samples, where the band at lower frequency with respect to the pure nitrile becomes more and more predominant.

The adsorption of oTN gives also rise to a CN stretching band shifted well above the value of the pure compound. The intensities of the bands of adsorbed oTN are well lower than those of the bands of adsorbed PrN, this agreeing with the fact that, due to its definitely higher size, the access of oTN in the MOR channels is highly, if not completely, hindered, so being essentially limited to the external surface and the pore mouths. Thus, the detection of the bands at 2240-2255  $\text{cm}^{-1}$  for oTN adsorbed on LiMOR, NaMOR and KMOR strongly suggests that alkali cations are also located at the mouth of the channels or well at the outer mordenite surface, and interact via the usual N-coordination, with oTN. The location of alkali ions at the outer surface also somehow agrees with the shift of the position of the OH stretching band of the silanol groups, thought to be located at the external surface, with the heaviest alkali cations  $\text{K}^+$  and  $\text{Cs}^+$ , both agreeing with a “perturbation” of the external mordenite surface by alkali cations.

In all cases, species characterized by CO and CN stretchings at lower frequency than the free molecule are also observed. In all cases these species appear to be more stable than the “usual” C-bonded (for CO) and N-bonded (for nitriles) species. This allows us to suppose that a different interaction occurs in this

case, and this interaction seems very likely to be “multiple”. Only in the case of nitriles adsorption on CsMOR the two species (N-bonded and “multiply” bonded) are difficult to be distinguished or resolved. The relative intensity of the two components, due to “usual C- or N- bonded species and for “multiply” bonded species, seem to indicate that the amount of multiply bonded species grows (at least relatively to that of the usual C- or N- bonded species) with the following trends: LiMOR < NaMOR < KMOR < CsMOR and CO < PrN < oTN. These trends indicate that this interaction is easier to be formed with larger cations, with more basic molecules (nitrile > CO) and at the external versus the internal surface (oTN > PrN). These data, together with those reported elsewhere for NaMOR interacting with other nitriles<sup>24</sup> and for CO and nitriles adsorbed on Na-FAU samples,<sup>25</sup> suggest that the possibility to find two interaction sites (likely two alkali cations) at the correct distance is a key factor for establishing this interaction. Very tentative structures for double interactions with two cations are reported in the scheme I.



**Scheme 1.** Tentative structures for CO and nitriles interacting with two cations.

The possibility of the interaction of CO with two cations has been considered previously by Ugliengo et al.<sup>41</sup> These authors considered the interaction of CO with couples of naked cations at various distances, and found these complexes

unstable. However, they did not exclude the possibility of formation of species interacting with two cations in the channels of zeolites. In fact, the electric field in the channels of alkali-zeolites, in spite of the predominance of the field generated by the cations, is also strongly influenced by the oxygen atoms and by the zeolite framework. This limits the possibility of displacement of the cations and also their net charges, and also provides additional components to the electric field. Although the needed calculations on this subject seem to be lacking, it seems to us that the “multiply bonded species” should primarily involve two cations, just because in the zeolite channels the most basic oxygens are actually shielded by the cations and this should hinder their direct interactions with CO and the CN bonds of nitriles.

On the other hand, the evidence for the formation of this “multiply bonded species”, that, when observed, are the most strongly adsorbed and the most resisting outgassing, tends to change the view of the chemistry of adsorption in zeolites. In fact, in previous studies only one site – one molecule or one site – two molecules interactions have been usually considered to occur and modeled in theoretical studies. In contrast, we show here that two sites – one molecule interactions may be very relevant. Adsorption on zeolites may appear as a cooperative action where the cavity plays a role not only as a host of the adsorption sites, but also as a unique environment where complex adsorption phenomena may occur.

### ***5.2.5. Acknowledgements***

The authors acknowledge the Generalitat of Catalunya for a grant (2002FI 00667).

### ***5.2.5. References***

- <sup>1</sup> Rege, S. U.; Yang, R. T.; Qian, K.; Buzanowski, M. A. *Chem. Eng. Sci.* **2001**, 56, 2745.
- <sup>2</sup> Méthivier, A. Separation of Paraxylene by Adsorption. In *Zeolites for cleaner technologies*; Guisnet, M.; Gilson, J. P.; Eds.; Imperial College Press: London, 2002, p. 209.
- <sup>3</sup> Castle, W. F. *Int. J. Refrigeration* **2002**, 25, 158.
- <sup>4</sup> Weitkamp, J.; Hunger, M.; Rymasa, U. *Micropor. Mesopor. Mat.* **2001**, 48, 255.
- <sup>5</sup> Davis, R. J. *J. Catal.* **2003**, 216, 396.
- <sup>6</sup> van Bokhoven, J. A.; Tromp, M.; Koningsberger, D. C.; Miller, J. T.; Pieterse, J. A. Z.; Lercher, J. A.; Williams, B. A.; Kung, H. H. *J. Catal.* **2001**, 202, 129.
- <sup>7</sup> Guisnet, M.; Gilson, J.P., Eds., *Zeolites for cleaner technologies*, Imperial College Press: London, Catalytic Science Series, Vol 3, 2002.
- <sup>8</sup> Moreau, F.; Ayrault, P.; Gnep, N. S.; Lacombe, S.; Merlen, E.; Guisnet, M. *Micropor. Mesopor. Mat.* **2002**, 51, 211.
- <sup>9</sup> Webster, C. E.; Cottone, A.; Drago, R. S. *J. Am. Chem. Soc.* **1999**, 121, 12127.
- <sup>10</sup> Yuvaray, S.; Chang, T. H.; Yeh, C. T.; *J. Phys. Chem. B* **2003**, 107, 4971.
- <sup>11</sup> Salla, I.; Salagre, P.; Cesteros, Y.; Medina, F.; Sueiras, J. E. *J. Phys. Chem. B* **2004**, 108, 5359.
- <sup>12</sup> Alberti, A.; Davoli, P.; Vezzalini, G.; *Z. Kristallogr.* **1986**, 175, 249.
- <sup>13</sup> Macedonia, M. D.; Moore, D. D.; Maginn, E. J.; Olken, M. M. *Langmuir*, **2000**, 16, 3823.
- <sup>14</sup> Devantour, S.; Abdoulaye, A.; Giuntini, J. C.; Henn, F. *J. Phys. Chem. B* **2001**, 105, 9297.

- <sup>15</sup> Maurin, G.; Senet, P.; Devantour, S.; Henn, F.; Giuntini, J. C. *J. Non-Crist. Solids* **2002**, 307-310, 1050.
- <sup>16</sup> Bell, R. G.; Devantour, S.; Henn, F.; Giuntini, J. C. *J. Phys. Chem. B* **2004**, 108, 3739.
- <sup>17</sup> Zecchina, A.; Otero Areán, C. *Chem. Soc. Rev.* **1996**, 25, 187.
- <sup>18</sup> Knözinger, H.; Huber, S. J. *Chem. Soc., Faraday Trans.* **1998**, 94 (15), 2047.
- <sup>19</sup> Hadjiivanov, K. I.; Vayssilov, G. N. *Adv. Catal.* **2002**, 47, 307.
- <sup>20</sup> Onida, B.; Bonelli, B.; Borello, L.; Fiorilli, S.; Geobaldo, F.; Garrone, E. *J. Phys. Chem. B* **2002**, 106, 10518.
- <sup>21</sup> Lamberti, C.; Bordiga, S.; Geobaldo, F.; Zecchina, A.; Otero Areán, C. *J. Chem. Phys.* **1995**, 103, 3158.
- <sup>22</sup> Bordiga, S.; Lamberti, C.; Geobaldo, F.; Zecchina, A.; Turnes Palomino, G.; Otero Areán, C. *Langmuir* **1995**, 11, 527.
- <sup>23</sup> Marie, O.; Massiani, P.; Thibault-Starzyk, F. *J. Phys. Chem. B* **2004**, 108, 5073.
- <sup>24</sup> Salla, I.; Montanari, T.; Salagre, P.; Cesteros, Y.; Busca, G. *J. Phys. Chem. B* **2005**, 109, 915.
- <sup>25</sup> Kozyra, P.; Salla, I.; Montanari, T.; Salagre, P.; Datka, J.; Busca, G. submitted paper
- <sup>26</sup> Bevilacqua, M.; Gutiérrez-Alejandre, A.; Resini, C.; Casagrande, M.; Ramírez, J.; Busca, G. *Phys. Chem. Chem. Phys.* **2002**, 4, 4575.
- <sup>27</sup> Bevilacqua, M.; Busca, G. *Catal. Commun.* **2002**, 3, 479.
- <sup>28</sup> Flanigen, E. M. In *Zeolite Chemistry and Catalysis*; Rabo J. A.; Ed.; ACS: Washington, 1979, p. 80

- <sup>29</sup> Geobaldo, F.; Lamberti, C.; Ricchiardi, G.; Bordiga, S.; Zecchina, A.; Turnes Palomino, G.; Otero Arean, C. *J. Phys. Chem.* **1995**, 99, 11167.
- <sup>30</sup> Tsyganenko, A. A.; Escalona Platero, E.; Otero Areán, C.; Garrone, E.; Zecchina, A. *Catal. Lett.*, **1999**, 61, 187.
- <sup>31</sup> Martra, G.; Ocule, R.; Marchese, L.; Centi, G.; Coluccia, S. *Catal. Today* **2002**, 73, 83.
- <sup>32</sup> Heise, H. M.; Winther, F.; Lutz, H. *J. Mol. Spectrosc.* **1981**, 90, 531.
- <sup>33</sup> Szymańska-Buzar, T.; Gowiak, T.; Czeluśniak I. *J. Organomet. Chem.* **1999**, 585, 215.
- <sup>34</sup> Montanari, T.; Bevilacqua, M.; Resini, C.; Busca, G. *J. Phys. Chem. B* **2004**, 108, 2120.
- <sup>35</sup> Ng, J. C. F.; Park, Y. S.; Shurvell, H. F. *Spectrochim. Acta A* **1992**, 48, 1139.
- <sup>36</sup> Quadri, S. M.; Shurvell, H. F. *Spectrochim. Acta A* **1995**, 51, 1355.
- <sup>37</sup> Becker, J. J.; Van Orden, L. J.; White, P. S.; Gagne, M. R. *Org. Lett.* **2002**, 4, 727.
- <sup>38</sup> Tretyakov, N. E.; Filimonov, V. N. *Kinet. Catal.* **1973**, 14, 803.
- <sup>39</sup> Deady, L. W.; Harrison, P. M.; Topsom, R. D. *Spectrochim. Acta A* **1975**, 31, 1665.
- <sup>40</sup> Chu, P. J.; Gerstein, B. C.; Nunan, J.; Klier, K. *J. Phys. Chem.* **1987**; 91; 3588.
- <sup>41</sup> Ugliengo, P.; Garrone, E.; Ferrari, A. M.; Zecchina, A.; Otero Arean, C. *J. Phys. Chem. B* **1999**, 103, 4839.

### **5.3. FT-IR Study of the adsorption of carbon monoxide and of differently hindered nitriles on Na-Faujasites: a confirmation for the formation of complex interactions**

#### ***Abstract***

The low temperature adsorption of CO and the room temperature adsorption of acetonitrile (AN), propionitrile (PN), isobutyronitrile (IBN) and pivalonitrile (PN) has been investigated on NaX (Si/Al at. ratio =1.3) and NaY zeolite (Si/Al at. ratio =2.4). The bands of CO adsorbed species on NaY have been reassigned. The relevance of Na<sup>+</sup> ions at S<sub>III</sub> or S<sub>III'</sub> positions also on NaY has been emphasized. Evidence is provided for the formation of complex interactions where nitrile molecules interact with more than one Na ions, like previously found on NaMOR.

### 5.3.1. Introduction

Sodium-Faujasites, in the form of either NaX or NaY, and other alkali-metal exchanged Faujasites are widely applied in the industry as selective adsorbants for gas mixture separation and gas purification, as well as catalysts, catalyst supports and catalyst components.<sup>1</sup>

Either in the form of powder packed beds or of membranes, alkali metal zeolites may allow the drying of air,<sup>2</sup> the separation of air's components ( $N_2/O_2$ ) by pressure/vacuum swing adsorption procedures,<sup>3</sup> the separation of  $CO_2$  from different gaseous streams,<sup>4</sup> the alkene/alkane,<sup>5</sup> the benzene/cyclohexane<sup>6</sup> and the xylene isomer separations.<sup>7</sup> The faujasite structure is constituted by quite wide supercages accessed through 12-member silicate rings with diameter near 0.74 nm, much smaller sodalite cages accessed through 6-member silicate rings and hexagonal prisms connecting the sodalite cages. Cations are located in different positions in the cavities depending on hydration-dehydration states or upon adsorption of different molecules.<sup>8,9</sup> The significant medium Lewis acidity of the alkali and alkali earth cations, increased by the loss of ligands in dry zeolites, is the key feature for the use of these materials as regenerable adsorbants. According to Davis,<sup>10</sup> that reviewed recently the perspectives of their use as catalysts, alkali-exchanged zeolites are considered to be solid base catalysts but their active sites should be envisioned as a combination of a Lewis acid and a Lewis base sites.

The low temperature adsorption of CO is today perhaps the most popular technique for Lewis acidity characterization but is also used for characterizing Brønsted sites of protonic zeolites by applying the H-bonding method.<sup>11-14</sup> The position of  $\nu_{CO}$  of adsorbed CO is shifted upwards on Lewis acidic  $d_0$  cations and on protonic sites as the result of a  $\sigma$ -type donation of the lone pair at the carbon atom, or of a simple polarization of the molecule. However, it has been

shown that also the O lone pair can be involved in a very weak O-bond interaction which shifts down the CO stretching frequency.<sup>15</sup> CO as a probe actually allows a very detailed analysis of the surface sites as they appear at low temperature without strong perturbations of the surface, having also free access to any cavity and avoiding steric hindrances. This is a good opportunity to evaluate “pure acidity”<sup>16</sup> but, it is also a drawback, because it does not provide information on the location of the sites in or out the different cavities of microporous materials. On the contrary, the use of sets of differently hindered nitriles may allow to discriminate between adsorption sites located in differently hindered sites or at the external surface in protonic<sup>17,18</sup> and cationic zeolites.<sup>19</sup> The interaction of basic molecules with the active sites in zeolites is generally modeled as being due to “one site-one molecule” interactions, or sometimes as “one site- two molecules” interactions. In the case of the adsorption of diatomic molecules on cationic zeolites, such as CO<sup>20</sup> and N<sub>2</sub><sup>21,22</sup> but also concerning the adsorption of nitriles, end-on  $\sigma$ -bonding interactions only are usually considered. In contrast, for olefins such as butenes<sup>23,24</sup> and pentenes<sup>25</sup> side-on  $\pi$ -bonding very likely occur.

Low temperature CO adsorption and hindered nitriles adsorption have been used recently to reexamine the adsorption sites of Na-Mordenite,<sup>26</sup> and in this case the formation of strongly adsorbed species interacting with more than one cation, possibly with a  $\pi$ -bonding additional to usual  $\sigma$ -bonding, or with a cation and an oxide ion has been proposed. The existence of complex interactions involving both cations and oxide species has also been proposed for ammonia adsorption on alkali-metal faujasites.<sup>27</sup>

Low temperature<sup>28-33</sup> and room temperature<sup>34</sup> IR studies of CO adsorption on alkali-metal faujasites have been published. In this paper we report on our re-examination of the CO- NaFAU system and on a new study on the adsorption

of hindered nitriles on NaX and NaY samples, in order to check if interactions similar to those observed on Na-MOR are detectable also on these systems.

### ***5.3.2. Experimental***

Zeolite NaY (Si/Al = 2.56) has been synthesized in the Institute of Industrial Chemistry of the Warsaw University while NaX zeolite (Si/Al = 1.31) has been synthesized in the Institute of Chemical Technology of the Jagellonian University in Krakow. CO cylinders were purchased from SIAD while the nitriles acetonitrile (AN), propionitrile (PrN), isobutylonitrile (IBN), pivalonitrile (PN), where pure products purchased from Aldrich.

Self-supporting pressed disks of pure zeolite powders were activated “in situ” in the IR cell by outgassing at 723 K before the adsorption experiments. The conventional gas manipulation/outgassing ramp was connected to a NaCl window- containing IR cell which allowed cooling by liquid nitrogen in an external jacket.

The adsorption/desorption process has been studied by transmission FT-IR. For nitriles, the adsorption procedure involves contact of the activated sample disk with vapors at room temperature at a pressure not higher than 2,5 kPa. The desorption process at increasing temperatures was performed in vacuum at temperatures compressed in the range 273 K and 573 K. CO adsorption was performed at 130 K (real sample temperature measured by a thermocouple) by the introduction of a known dose of CO gas. IR spectra were collected evacuating at increasing temperatures between 130 and 273 K.

### **5.3.3. Results**

#### **5.3.3.1. Low temperature CO adsorption on NaX and NaY**

The overall spectra of activated NaX sample in the OH stretching region, a weak sharp band at  $3684\text{ cm}^{-1}$  that does not correspond to the OH stretching of the bridging hydroxy groups of NaHX zeolite.<sup>35</sup> This weak feature, observed frequently on NaX samples<sup>25</sup> is likely associated to traces of residual water molecules.<sup>37</sup> In the case of the NaY, the spectrum shows only a sharp band at  $3739\text{ cm}^{-1}$ . This band can be assigned to the OH stretching of terminal silanol Si-OH groups located at the external crystal surface or in structural defects. In both cases no evidence is found for bridging OH's (typically found in the range  $3650\text{-}3550\text{ cm}^{-1}$  in proton-containing zeolites), showing that cation exchange is complete.

Figure 1 shows the IR bands of CO adsorbed at low temperature on NaX zeolite. At temperatures lower than 163 K mainly one asymmetric and very intense (maximum out of scale) band is observed on the CO stretching range. With outgassing at increasing temperatures, the intensity of this band diminishes its main maximum being found at  $2165\text{ cm}^{-1}$  with a shoulder at  $2176\text{ cm}^{-1}$ . Additionally, other two bands with very weak intensity, located at  $2138\text{ cm}^{-1}$  and  $2115\text{ cm}^{-1}$  are present. By progressively increasing temperature upon outgassing, the main band together with its shoulder (that at the lowest coverages shifts up to  $2182\text{ cm}^{-1}$ ) parallelly decrease their intensity, while the two lower frequency components disappear even earlier. Our spectra look very similar to those reported by Martra et al.<sup>33</sup> while they seem distinctly different from that reported by Hüber and Knözinger<sup>31</sup> at 0.1 hPa at 88 K on a NaX sample closely similar to our.

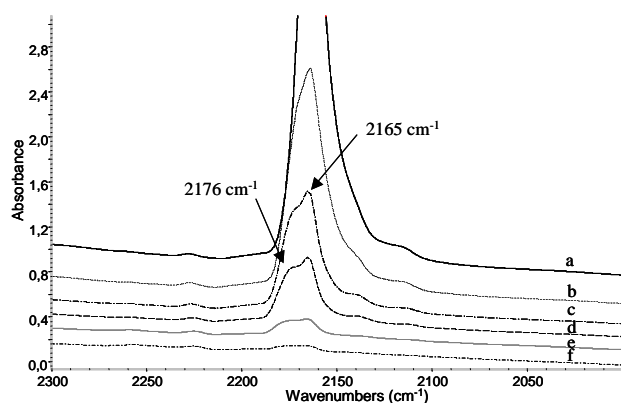


**Figure 1.** FT-IR spectra of activated NaX in the presence of CO gas under evacuation at 163K (a), 173K (b), 183 K (c), 193 K (d), 203 (e) and 213 K (f) in the CO stretching range.

As it is well known, four predominant locations have been found for Na<sup>+</sup> ions in the Faujasite framework. The S<sub>I</sub> and S<sub>F</sub> sites, that are in the center of the hexagonal prisms and near the six-fold mouth inside the sodalite cages, respectively, are considered to be not accessible to CO. The S<sub>II</sub> site and S<sub>III</sub> sites are near the walls of the supercage, at the center of six-fold and four-fold mouths, respectively. Martra et al.<sup>30</sup> assigned the main band they found at 2164-7 cm<sup>-1</sup> to CO C-bonded to S<sub>II</sub> site cations, while the shoulder they report at 2177-5 cm<sup>-1</sup> has been assigned to CO C-bonded to S<sub>III</sub> site cations. In contrast, Hüber and Knözinger<sup>31</sup> found the most intense band at 2166 cm<sup>-1</sup>, they assigned to CO C-bonded to S<sub>III</sub> site cations, with a shoulder at 2157 cm<sup>-1</sup> assigned to CO C-bonded to S<sub>II</sub> site cations.

The band at 2139 cm<sup>-1</sup> disappears completely quite fast in vacuum and therefore can be attributed with confidence to pseudo-liquid physisorbed CO inside the zeolite pores. The band at 2115 cm<sup>-1</sup> can be attributed to O-bonded

CO species ( $\text{Na}^+ \cdots \text{OC}$ ) although, as noted by Martra et al.<sup>33</sup> C-bonded  $^{13}\text{CO}$  and a component of sodium-dicarbonyl species may participate to it.

The spectra of the IR bands of adsorbed CO on NaY zeolite are shown in Figure 2.

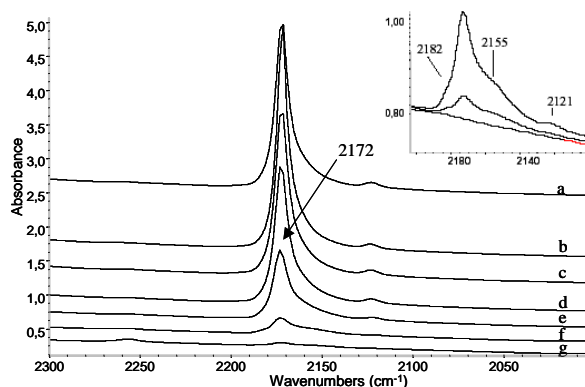


**Figure 2.** FT-IR spectra of activated NaY in the presence of CO gas under evacuation at 133K (a), 143K (b), 153 K (c), 163 K (d), 173 (e), 193 K (f) and 203 (g) in the CO stretching range.

We observe an intense and asymmetric band with the main maximum at 2172  $\text{cm}^{-1}$  and a weak band at 2123  $\text{cm}^{-1}$ . Only by expanding the weak spectra recorded after outgassing at 193 and 203 K (look at the inset in Figure 2) become evident two additional components, one at lower frequency the other at higher frequency, in the main peak namely at 2182 and near 2155  $\text{cm}^{-1}$ . Hüber and Knözinger<sup>29</sup> found a similar spectrum with four components and attributed them to CO C-bonded on  $\text{S}_{\text{II}}$  sites near six-fold ring having one, two (meta), two (para) and three Al ions. The approach of Hüber and Knözinger,<sup>31</sup>

which also based on the Na and Al distribution between the different sites as deduced from NMR and XRD data, seems questionable to us, due to the exceeding intensity of the band at 2172 cm<sup>-1</sup>. This band is in fact attributed to CO C-bonded to Na ions on S<sub>II</sub> sites near two Al-containing six-fold rings, but this species should not be so more likely than the others. Also in this case, the band at 2123 cm<sup>-1</sup> can be attributed to very weakly bonded CO possibly like Na<sup>+</sup> ⋯ OC.

Therefore, neither on NaX nor on NaY we have been able to find low-frequency but strongly adsorbed CO species. We can conclude that multiply-bonded CO like that formed on Na-MOR<sup>26</sup> cannot be found on Na-FAU, possibly because of the larger dimensions of the supercages of the FAU structure, which prevents the cations responsible for the “multiple interaction” to be near enough to establish this interaction.

### ***5.3.3.2. Adsorption of acetonitrile and propionitrile on NaX and NaY***

Acetonitrile (AN) and propionitrile (PrN) adsorption can be used for characterizing adsorbing sites in zeolites. Both molecules do not have relevant steric hindrance and can interact with all adsorption sites in the case of mordenite samples.<sup>18,26</sup> The adsorption of AN on NaX and NaY has already been reported.<sup>25,37</sup> It is well known that the AN C≡N triple bond stretching mode gives rise to two bands due to the Fermi Resonance between the fundamental stretching CN with a δCH<sub>3</sub> + νC-C combination. Both components shift upwards the more the stronger in the electronwithdrawing power of the cations to which the nitrile coordinates. The Fermi Resonance doublet for AN in CCl<sub>4</sub> solution is observed at 2292, 2255 cm<sup>-1</sup> (Figure 3a.). On both NaX (Figure 3b-d, left) and NaY (Figure 3e-g, right) the bands tend to

shift further upwards by increasing outgassing temperature, i.e. by decreasing coverage. The final position is found at slightly higher wavenumbers for NaY (2300, 2270  $\text{cm}^{-1}$ ) than for NaX (2297, 2268  $\text{cm}^{-1}$ ) and this could be associated to a slightly higher Lewis acidity, i.e. a slightly lower electron density, for the most acidic  $\text{Na}^+$  ions on NaY with respect to NaX. In both cases, however, upon outgassing a further band appears at lower frequencies that apparently are due to a species that resists outgassing more. These bands are found at 2237  $\text{cm}^{-1}$  on NaX and at 2246  $\text{cm}^{-1}$  on NaY, and resemble that found at 2238  $\text{cm}^{-1}$  on Na-MOR,<sup>26</sup> assigned to “multiply bonded” species.

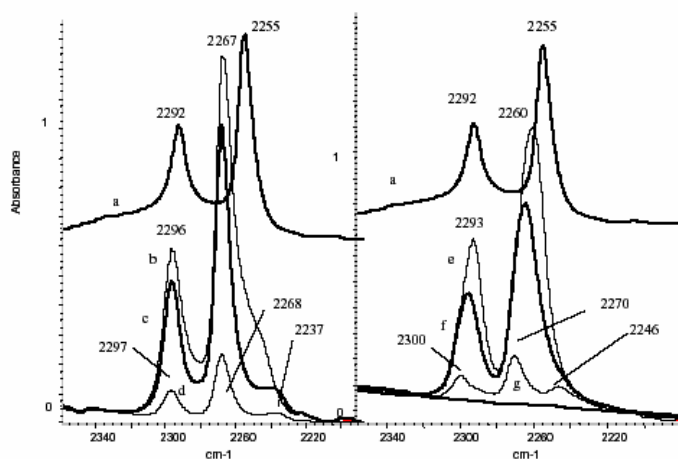


**Figure 3.** FT-IR spectra of AN in  $\text{CCl}_4$  solution (a), NaX in the presence of AN vapors after evacuation at 373 K (b), 423 K (c) and 473 K (d), NaY in the presence of AN vapors after evacuation at 300 K (e), 373 K (f) and 423 K (g).

The spectra of PrN adsorbed on NaX and NaY samples, and after outgassing at different temperatures, are shown in Figures 4 and 5, respectively. The nitrile spectrum on  $\text{CCl}_4$  solution, used as a reference, is also shown. From the subtracted spectra of PrN adsorbed on NaX after evacuation at room

temperature (Figure 4b) a broad band is observed at 2250  $\text{cm}^{-1}$  on the CN stretching region. By heating at 373 K under vacuum, this band starts to resolve into two with maxima at 2256 and 2246  $\text{cm}^{-1}$ . Finally, after the desorption process at 423 K and 473 K (Figure 4d-e), two bands are observed with the maxima at 2262 and 2228  $\text{cm}^{-1}$ . The main band at the lowest coverages is found at similar wavenumbers than on Na-MOR<sup>26</sup> but is indicative of the PrN interaction with Na ions through the N lone pair. The lower frequency band, instead, is similar but at a definitely lower wavenumber with respect to that found on Na-MOR<sup>26</sup>, and assigned to a “multiply bonded” species.

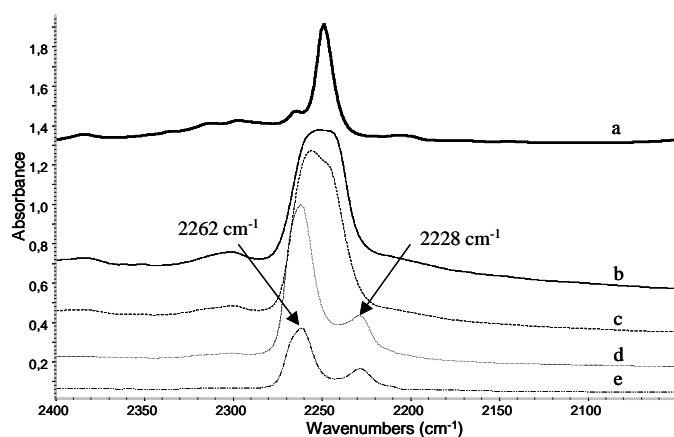


**Figure 4.** FT-IR spectra of PrN in  $\text{CCl}_4$  solution (a), NaX in the presence of PrN vapors after evacuation at room temperature (b), at 373 K (c), 423 K(d) and 473 K (e).

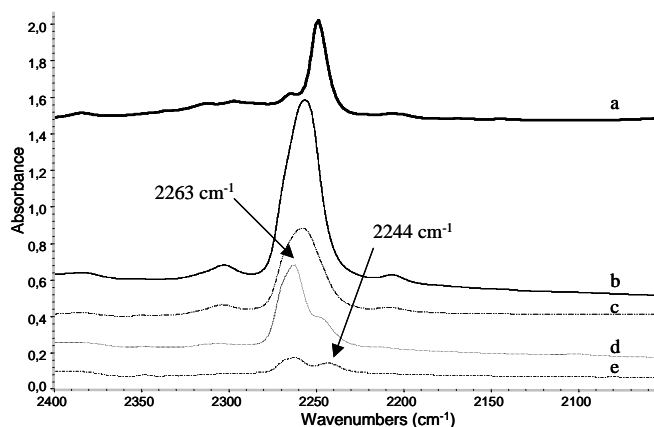


**Figure 5.** FT-IR spectra of PrN in  $\text{CCl}_4$  solution (a), NaY in the presence of PrN vapors after evacuation at room temperature (b), at 373 K (c), 423 K (d) and 473 K (e).

A more detailed analysis of the CN stretching region can be made by analyzing the spectra obtained by subtracting from the band obtained in every step the spectrum of the step before (Figure 6). This shows that the main band shifted upwards with respect to that of the same compound in solution actually contains at the lowest coverages at least two components (2269, 2263  $\text{cm}^{-1}$ ) but that the main feature still present after outgassing at 373 K is still located near 2247  $\text{cm}^{-1}$  with a fourth component near 2252  $\text{cm}^{-1}$ . Interestingly, upon outgassing at 373 K the absorption at 2245-2253  $\text{cm}^{-1}$  decreases in intensity while that at 2263 and 2269  $\text{cm}^{-1}$  increases in intensity. In practice it seems clear that some propionitrile molecules displace from weaker to stronger adsorption sites, and that the two families (weaker and stronger sites, possibly due to  $\text{Na}^+$  ions at  $S_{\text{II}}$  and  $S_{\text{III}}$  or  $S_{\text{III}'}$  respectively) are both double (i.e. composed by two different species).

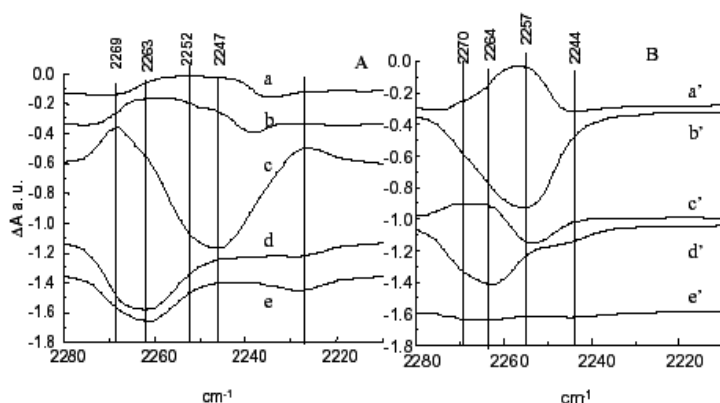


**Figure 6A and B.** Subtraction spectra from Figure 4 and Figure 5, a and a': evac. at r. t. – in the presence of the vapour, b and b': evac. at 373K- evac at r.t., c and c' evac. at 423K- evac 373 K, d and d': evac. at 473 K- evac. at 423K, e and e': evac. 523K – evac. 473 K.

A parallel situation is found for PrN on NaY (Figure 5). From the subtracted spectra of PrN adsorbed on NaY after evacuation at room temperature and at 373 K (Figure 5b-c) a broad band with the main maximum at  $2258\text{ cm}^{-1}$  is observed on the CN stretching region. By heating at 423 and 473 K under vacuum (Figure 5d-e), also in that case a new band at lower frequencies appears. Thus two bands at  $2263$  and  $2244\text{ cm}^{-1}$  are observed again. On NaY, however, the lower frequency band is relatively less shifted down than on NaX.

The analysis of the subtraction spectra (Figure 6B) shows that at the lowest coverages the bands on NaY and on NaX are very similar, for both position and relative intensity. Otherwise, at higher coverages, the main band on NaY is at higher frequencies than on NaX ( $2255\text{ cm}^{-1}$  with respect to  $2245\text{--}2253\text{ cm}^{-1}$ ). All features are actually shifted a little bit upwards on NaY than on NaX. This parallelism supports the assignment of the two features to the nitrile adsorbed on  $\text{Na}^+$  ions at  $\text{S}_{\text{II}}$  and  $\text{S}_{\text{III}}$  or  $\text{S}_{\text{III}'}$  respectively. If this is true, the existence and

activity of well defined Na<sup>+</sup> sites at S<sub>III</sub> or S<sub>III'</sub> also in the case of NaY should be confirmed.

### ***5.3.3.3. Adsorption of isobutyronitrile and pivalonitrile on NaX and NaY***

Isobutyronitrile (IBN) and pivalonitrile (PN) are more hindered nitriles, whose access to the mordenite “side pockets” was found to be partially forbidden.<sup>18, 26</sup> They have been used here to check if hindering of the access to Na ions in Faujasites can be found.

The subtracted spectra obtained for NaX sample using isobutyronitrile (IBN) and pivalonitrile (PN) vapors as probe molecules are shown in Figures 7 and 8, respectively. On the spectra of IBN adsorbed on NaX and evacuated at room temperature a broad band centered at 2247 cm<sup>-1</sup> can be observed (Figure 7b). When increasing the outgassing temperature to 373 K, this band becomes narrower with the maximum at 2253 cm<sup>-1</sup> and a shoulder at 2244 cm<sup>-1</sup> (Figure 7c). By still increasing temperature the intensity of the band diminishes and two bands are observed at 2259 and 2228 cm<sup>-1</sup> (Figure 7d-e).

The behaviour observed for the spectra of PN adsorbed on NaX is similar to that observed for IBN on the same zeolite. After PN adsorption on NaX since a broad band centered at 2239 cm<sup>-1</sup> is observed when evacuating at room temperature (Figure 8b). When increasing the outgassing temperature to 373K, a shoulder at 2234 cm<sup>-1</sup> starts to appear (Figure 8c), and finally, at the desorption temperature of 473 K, the spectrum shows two bands with the maxima at 2250 and 2223 cm<sup>-1</sup> (Figure 8d). Thus, after both IBN and PN adsorption/desorption on NaX, a band at frequencies lower than the frequency of the corresponding solution nitrile spectra is observed (Figures 7a and 8a), and these bands show a higher resistance to the desorption process.

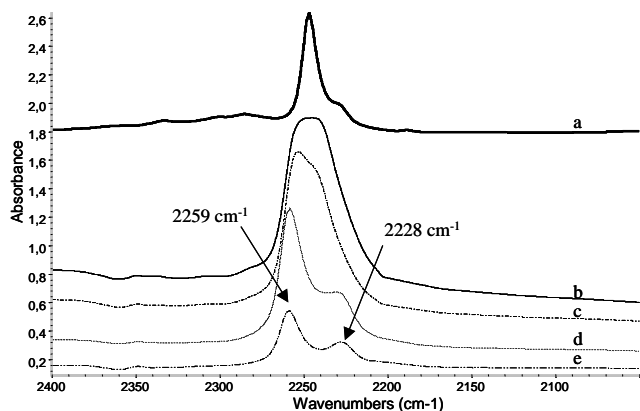


**Figure 7.** FT-IR spectra of IBN in  $\text{CCl}_4$  solution (a), NaX in the presence of IBN vapors after evacuation at room temperature (b), at 373 K (c), 423 K(d) and 473 K (e).

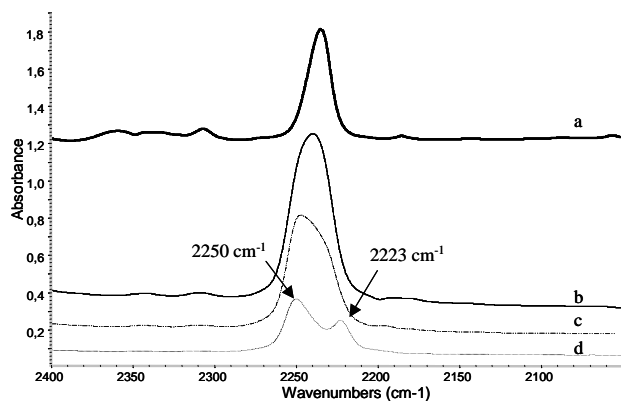


**Figure 8.** FT-IR spectra of PN in  $\text{CCl}_4$  solution (a), NaX in the presence of PN vapors after evacuation at room temperature (b), at 373 K (c), and 473 K (d).

The subtracted spectra obtained for NaY sample using isobutyronitrile (IBN) and pivalonitrile (PN) vapors as probe molecules are shown in Figures 9 and 10, respectively. In both cases the spectra obtained are similar, one asymmetric band with a tail to lower frequencies is observed, well shifted above than the band for the free nitrile. In the case of IBN this band is centered at  $2258\text{ cm}^{-1}$

and in the case of PN this band is centered at  $2251\text{ cm}^{-1}$ . These bands decrease in intensity and become narrower when temperature increases on evacuation. So, in the case of IBN and PN adsorption on NaY we have not observed the band at lower frequencies than the liquid nitrile spectrum.

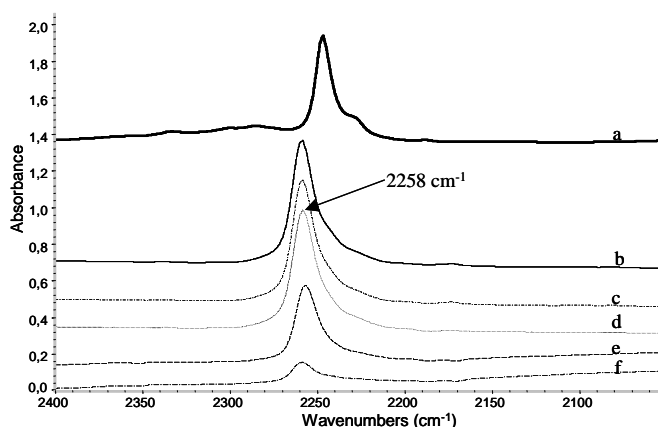


**Figure 9.** FT-IR spectra of IBN in  $\text{CCl}_4$  solution (a), NaY in the presence of IBN vapors after evacuation at room temperature (b), at 373 K (c), 423 K(d), 473 K (e) and 523 (f).

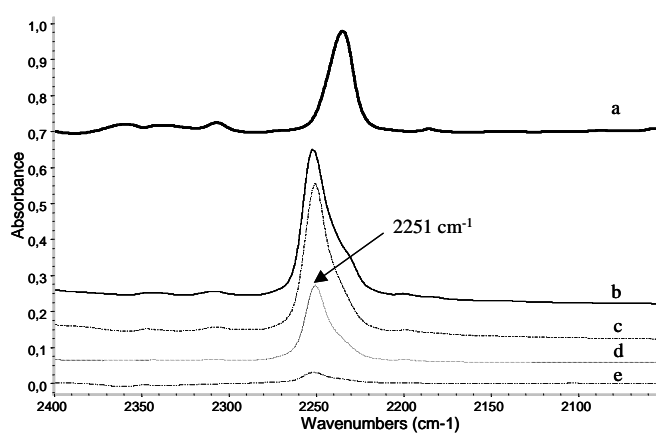


**Figure 10.** FT-IR spectra of PN in  $\text{CCl}_4$  solution (a), NaY in the presence of PN vapors after evacuation at room temperature (b), at 373 K (c), 423 K(d) and 473 K (e).

An analysis of the subtraction spectra relative to the adsorption of the most hindered nitrile PN on NaX and NaY (Figure 11) can give some further information on the multiplicity and distribution of Na<sup>+</sup> sites. It seems that this hindered nitrile gives rise to less resolved bands but the maximum shifts more continuously from near 2240 to 2250 cm<sup>-1</sup> on NaX and that the position is nearly the same also on NaY.

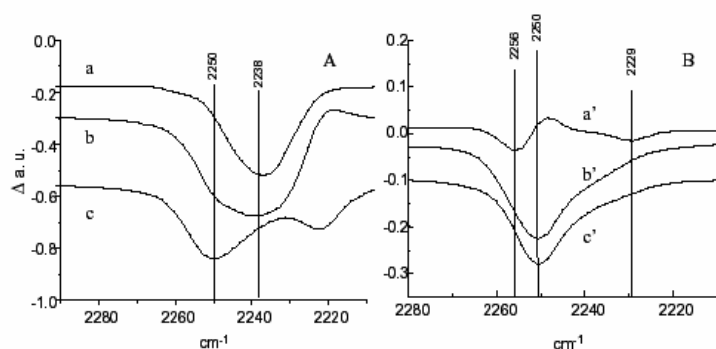


**Figure 11A and B.** Subtraction spectra from Figure 8 and Figure 10, a and a': evac. at r. t. – in the presence of the vapour, b and b': evac. at 373K- evac at r.t., c and c' evac. at 423K- evac 373 K,

### 5.3.4. Discussion.

#### 5.3.4.1. Adsorption sites and $\sigma$ -bonded CO adsorbed species

The sodium distribution in anhydrous NaX and NaY has been the object of several studies.<sup>8,9,38,39</sup> Although other possible locations have been considered by different authors, an idealized (and slightly simplified) model for NaX

Faujasite with a Si/Al ratio of 1, having for the unit cell the formula  $\text{Na}_{96}\text{Si}_{96}\text{Al}_{96}\text{O}_{384}$ , implies a 100 % occupation of the 32 so-called  $S_{\text{I}}$  sites which are located inside the sodalite cage in front of the 6-ring window connected to the hexagonal prism, the 100 % occupation of the 32  $S_{\text{II}}$  sites which are located in the middle of the 6-ring window connecting the supercage and the sodalite cage, and the 66 % occupation of the 48  $S_{\text{III}}$  sites, which are a little displaced towards inside the supercage, near the middle of the 4-rings separating them from the sodalite cage.<sup>9</sup> Other authors<sup>8</sup> consider the presence of 32  $\text{Na}^+$  ions in one third of the  $S_{\text{III}}$  sites (instead of the  $S_{\text{III}}$  sites), located in the 12-ring windows of the supercage. By decreasing the Al and the sodium contents<sup>9</sup> (so shifting from NaX to NaY) the occupancy of sites  $S_{\text{I}}$  and  $S_{\text{III}}$  decreases while sites I (located just in the middle of the hexagonal prisms) become populated. For a Si/Al of 3 (i.e. with a formula  $\text{Na}_{48}\text{Si}_{144}\text{Al}_{48}\text{O}_{384}$ ), sites  $S_{\text{I}}$  and  $S_{\text{II}}$  are fully populated, while  $S_{\text{I}}$  and  $S_{\text{III}}$  are empty.

According to most authors, sites I and I', which are inside the sodalite cage and of the hexagonal prisms, respectively, should be inaccessible to adsorbates. So adsorption is expected to occur only in the supercage. Every supercage may contain up to 8 Na ions: four cations at  $S_{\text{II}}$  and four cations at  $S_{\text{III}}$  (or  $S_{\text{III}}$ ) for Si/Al = 1, while only the four cations at  $S_{\text{II}}$  for Si/Al = 3. In the case of our samples, characterized by Si/Al ratios of 1.31 and 2.56, the Na cation distribution should be not very different from those considered for the ratios Si/Al = 1 and 3, respectively.

In NaX  $\text{Na}^+$  ions in  $S_{\text{III}}$  sites are expected to present a higher positive charge than those at  $S_{\text{II}}$ , so the Lewis acidity of cations at  $S_{\text{III}}$  is expected to be the greatest.<sup>29</sup> Also cations located in  $S_{\text{III}}$  sites,<sup>8</sup> if any, should be more Lewis acidic than those in  $S_{\text{II}}$ . In agreement with this, and with previous authors, we assign the bands at 2176 and 2165  $\text{cm}^{-1}$  observed after low temperature CO adsorption on NaX to carbonyls on  $\text{Na}^+$   $S_{\text{III}}$  (or  $S_{\text{III}}$ ) and  $S_{\text{II}}$  cations,

respectively. This also agrees with the relative intensity of the observed bands where the band attributed to carbonyls on S<sub>III</sub> ions is less intense at saturation than that attributed to carbonyls on S<sub>II</sub>, in agreement with a S<sub>III</sub>/S<sub>II</sub> well lower than 1 in our sample whose composition is near Na<sub>55</sub>Si<sub>137</sub>Al<sub>55</sub>O<sub>384</sub>.

As for the assignment of the bands associated to CO adsorbed on NaY, the main band observed at 2172 cm<sup>-1</sup> is quite easily attributed to carbonyls on Na<sup>+</sup> ions located in site S<sub>II</sub>, which is expected to be largely predominant. The shift to higher frequency of this species on NaY with respect to NaX (for sites at S<sub>II</sub>) should indicate that oxygen species in the six-ring windows near S<sub>II</sub> are a little less basic on NaY than on NaX, according to the lower Al content in the framework. The expansion of the spectra recorded at very low coverages allows to evidence two other components here, but very weak, at 2182 and at 2155 cm<sup>-1</sup>. In their previous work, Marra et al.<sup>29</sup> found only the main band. Hüber and Knözinger<sup>31</sup> and Vayssiliov et al.<sup>30</sup> instead, found, besides the main one at 2172 cm<sup>-1</sup>, three other at 2182, 2165, 2155 cm<sup>-1</sup>. They assigned those four bands to Na<sup>+</sup>-carbonyls on four different S<sub>II</sub> sites associated to different Al contents and positions. This assignment has also been given by Tsyganenko et al.<sup>32</sup> This assignment seems however to be inconsistent, in our opinion, with the exceedingly strongest intensity of the component at 2172 cm<sup>-1</sup> observed at saturation. On the other hand, the composition of our sample (which is actually the same of that of the sample used in references 30 and 31) that corresponds to a formula near Na<sub>55</sub>Si<sub>137</sub>Al<sub>55</sub>O<sub>384</sub>, is such that occupancy of site III should be still not nil. So, the band at 2182 cm<sup>-1</sup> can reasonably be due to Na<sup>+</sup> carbonyls on residual S<sub>III</sub> sites. Consequently, the band assigned to CO on S<sub>II</sub> cations should be almost insensitive to the number of Al ions in the 6- rings. As for the feature observed at 2155 cm<sup>-1</sup>, it seems evident that it is due to a species which are in very small amounts but more strongly bonded than that characterized by the band at 2172 cm<sup>-1</sup>. In fact, outgassing tend to cause the disappearance of the band at 2172 cm<sup>-1</sup> but leaves more evident the band at 2155 cm<sup>-1</sup>. Here we

found a species that appears to be less shifted upwards but less resistant to outgassing than the usual  $\text{Na}^+$  carbonyls. This may be due either to diffusional effects (the desorption is hindered in some way) or to the existence of a different interaction. From these considerations, we can propose two different assignments for this species, either to terminal carbonyls on  $\text{Na}^+$  ions located in the interior of the sodalite cage or of the hexagonal prisms, whose desorption could be hindered by the small dimensions of the cavity windows, or, alternatively, to multiply bonded species on the supercage. However, the lack of detection of this species on  $\text{NaX}$  (in whose supercage much more  $\text{Na}^+$  ions are present) allows us to rule out this second possibility. It seems to us possible that few CO molecules, whose van der Waals radius is not far from the half of the diameter of six ring windows, could find the way to enter the sodalite cavities (perhaps through defective sites) and to produce carbonyls on  $\text{Na}^+$  located at  $S_{\text{I}}$  sites.

#### ***5.3.4.2. “Usual” $\sigma$ -bonded nitrile adsorbed species***

As shown in Table 1 and in Figures 3-11, the adsorption of all nitriles gives rise to bands located well above the frequency of the free molecule, that may be assigned to “usual”  $\sigma$ -bonded nitrile adsorbed species on  $\text{Na}^+$  ions. The analysis of the behaviour of these bands allows us actually to observe several components that are certainly related to a remarkable heterogeneity of the available  $\text{Na}^+$  ions. If the exact position of the components for adsorbed AN is difficult, due to the presence of the Fermi Resonance doublet, for PrN, IBN and PN three or four different adsorbed species may be observed. The comparison allows to suggest that the bands at higher frequencies can be assigned to nitrile molecules adsorbed on the most electron poor  $\text{Na}^+$  cations located at  $S_{\text{III}}$  or  $S_{\text{III}'}$  sites, while the less perturbed nitrile species should be due to the more abundant  $\text{Na}^+$  cations located at  $S_{\text{II}}$  sites. This means that the

existence and relative importance of Na<sup>+</sup> cations located at S<sub>III</sub> or S<sub>III'</sub> sites should be not negligible, in agreement with the more recent data concerning the distribution of Na ions in Na Y zeolite.

**Table 1.** Position of the IR bands (cm<sup>-1</sup>) of adsorbed nitriles and CO on Na-MOR, NaY and NaX.

Adsorbed molecule	Na-MOR	NaX	NaY	Free molecule
CO			2182	
	2175	2176	2172	
	2164	2165	2155	
	2138	--	--	2143 (gas)
AN	2299	2297	2293-2300	2292
	2268	2268	2260-2270	2255
	2248	2237	2246	
PrN	2267	2269-2263	2270-2264	
		2252-2247	2255-2253	2249
	2241	2228	2244	
IBN	2260	2265-2245	2265-2252	2247
	2235	2228	--	
PN	2253	2250-2237	2256-2250	2235
	2221	2223	--	

A rough evaluation of the amount of adsorbed nitriles on NaX and NaY shows that adsorbed species are definitely more abundant on NaX than on NaY, while that there is not much difference between the different nitriles adsorbed in the same solid. So the amount of adsorbed species depends on the amount of Na<sup>+</sup> ions in the supercage, while steric hindrance is not so important, due to the sufficiently large size of this cage.

### 5.3.4.3. “Unusual” low frequency nitrile adsorbed species

The data reported here may be discussed in parallel with those have been published recently concerning the adsorption of CO and several nitriles on NaMOR zeolite in the same conditions.<sup>26</sup> Over NaMOR we found for both CO and the nitriles the unusual formation of bands at lower frequencies with respect to the free molecule but resisting outgassing more than the “usual” species characterized by bands at higher frequencies than the free molecules. This behavior was interpreted assuming that these “unusual” species are involved in multiple or complex interactions, involving either more than one cation or one cation and one oxygen atom.

The possibility of the formation of these strongly bonded species also on NaX and NaY is determined here and, finally, this confirms that this is a newly discovered but potentially very relevant kind of interaction. The spectroscopic evidence of the formation of such species actually gives a new light to the chemistry of cationic zeolites, where the formation of “two-sites – one molecule” adsorbate – adsorbant interaction (usually taken into account) must be considered possibly as the more determinant one.

In reference 26 the low frequency, strong interaction species were supposed to be due either to interaction with more than one cation or to a complex interaction involving one cation and one basic oxygen. In the case of NaX samples with Si/Al = 1, every supercage, which is near a sphere with 13 Å diameter, contains 8 Na<sup>+</sup> ions, four at S<sub>II</sub> and four at S<sub>III</sub> or S<sub>III'</sub> the data of Buttefey et al.<sup>39</sup> indicate that most Na ions should actually be displaced from the S<sub>III</sub> crystallographic position significantly (~ 1 Å), and that some of them are displaced very much until the S<sub>III'</sub> crystallographic position. The distance between two S<sub>II</sub> sites is 7.69 Å<sup>40</sup> while the distance between a S<sub>II</sub> and a S<sub>III</sub> or S<sub>III'</sub> crystallographic site may be as low as 4.5-5.5 Å.<sup>41</sup>

The possibility of forming species where interaction involves both the Na cation and the oxygen to which the same ion is also bonded, like proposed to occur with ammonia on NaX, seems unlikely for the much larger nitrile molecules. On the other hand, the possibility of weak interactions of the C-H bonds of nitriles with other oxygen atoms exposed in the cavity, like proposed to occur for hydrochlorocarbons in Na-Faujasites<sup>42</sup> should not cause a decrease in the CN stretching frequency. Taking into account that the cations may displace a little bit upon adsorption of different molecules, the possibility of the formation of adsorbed species where two different cations interact with the N lone pair and with a  $\pi$ -type orbital seems to be possible on NaX. The more difficult detection of such species on NaY, where we can find it for the unhindered nitriles AN and PrN, unlike the hindered nitriles IBN and PN, is logical due to the much lower occupancy of S<sub>III</sub> and/or S<sub>III</sub> sites in this case, and to the less easy accommodation of the hindered and rigid nitrile molecules PN and IBN, with respect to AN and PrN.

Another interesting feature is that the shift down of the CN stretching frequency is definitely stronger on NaX ( $\sim 20\text{ cm}^{-1}$ ) than on NaY and Na-MOR ( $\sim 5\text{-}12\text{ cm}^{-1}$ ) for AN, PrN and IBN, while it is similar on NaX and Na-MOR for PN. ( $\sim 13\text{ cm}^{-1}$ ). Due to the lower Al and sodium contents on NaMOR (Si/Al 6.5) and NaY than on NaX, we may conclude that the predominant Na-Na distance of the nearest cations is definitely larger on NaMOR (and NaY) than on NaX, so in the last solid this interaction may be stronger at least for the less sterically demanding nitriles.

The abundance of this “unusual” interaction may be measured by using the ratio (R) of the bands of “unusual strongly bonded species” / “usual  $\sigma$ -bonded species”. This ratio is definitely larger on NaMOR when hindered nitriles are considered (like PN, or also benzonitrile and orthotoluonitrile) than when unhindered nitriles (like AN and PrN) are taken into account, just in contrast to

what happens on NaY. Consequently, it seems very likely that these interactions mostly occur in or at the mouth of the main channels in the case of NaMOR, where the more hindered nitrile should not penetrate. The above defined ratio (R) is definitely larger for NaMOR<sup>26</sup> than for NaX at least for PN and IBN, and this may be related to the larger size of the Faujasite supercage windows with respect to the Mordenite main channels. Thus this interaction should be limited at the external surface for NaMOR but should occur in the supercages for NaFAU, where the “usual” interactions also occur and are very abundant.

This “unusual” interaction is observed on NaX and NaY for nitriles but not for CO. This may be associated to the exceeding weakness of the basicity of CO with respect to that of the nitrile molecules (proton affinity 598 versus 783 kJ/mol, for acetonitrile). Alternatively, it may be due to the quadrupolar nature of CO (where the oxygen is formally positively charged) with respect to the polar nature of the C≡N triple bond, which finally results in a lower availability of  $\pi$ -type orbitals of CO to interact to a further No ion with respect to nitriles.

In any case this result evidences one of the limits in the use of CO as a probe molecule for zeolite adsorption sites, as discussed elsewhere.<sup>43</sup> Also in this case CO, due to its weakness as a base and its very low dimension fails in giving information on effects which are more or less cooperative and spatially demanding.

### ***5.3.5. Conclusions***

The study of CO adsorbed at low temperature and of a set of differently hindered nitriles adsorbed on NaX and NaY zeolites allows to obtain some new information on the sites available for these materials which are relevant in

industrial adsorption and catalysis processes. In particular we modified the assignments given in the literature to the features of CO adsorbed on NaY zeolite.

Our data show that two types of adsorbed species are well evident: i) simply coordinated species via a Lewis acid-base interaction. ii) multiply bonded species.

The typical single coordination of CO through the C atom lone pair to Na<sup>+</sup> cations is well evident and has been the object of several previous investigations. However, the data reported here allow to modify significantly the previous assignments for CO adsorbed on NaY. Our data in fact indicate that the existence and the role of Na<sup>+</sup> cations at S<sub>III</sub> or S<sub>III'</sub> sites is not negligible on NaY, even if they have lower population than on NaX, as shown by diffraction and model studies. We found here features that are assigned to CO and nitriles adsorbed on such ions. These species are the most strongly bonded and, consequently, they may be the more relevant from the points of view of catalysis and adsorption. So, although the S<sub>III</sub> or S<sub>III'</sub> positions are expected to be empty for NaY having Si/Al atomic ratio of 3, they are populated for samples whose Si/Al atomic ratios lower than 3, and they could become the more relevant in this case. Nitrile adsorbed species allow us to conclude that both families of sites, at S<sub>II</sub> and at S<sub>III</sub> or S<sub>III'</sub> positions, are actually heterogeneous possibly due to the different number of Al ions present in the neighbors.

O-bonded adsorbed CO species are also observed, like emphasized in previous studies. They give rise to very weakly adsorbed species that should not be very relevant in practice just because of their weakness.

On the other hand, nitrile adsorption allows to show the formation on NaX and NaY, like on NaMOR, of multiply bonded species. These species are the most strongly bonded, so in principle they could be the most relevant in

adsorption and catalysis. They are formed with nitriles but not with CO on NaX and NaY, possibly due to the less basic character of CO with respect to nitriles. The detection of such species with nitriles unlike CO shows one of the limits of the use of CO as a probe for surface characterization.

The multiply bonded species are observed on NaY only when the less hindered nitriles are used. This may be due to a greater difficulty to find the right geometry to build up this interaction when the amount of Na cations is small (as for NaY) and the nitrile is hindered. This agrees with the observation, made on NaMOR but likely correct also for Na-FAU, that the formation of this interaction is activated (i.e. it needs a slight warming).

### ***5.3.6. Acknowledgements***

P.K., J.D. and G.B. acknowledge the grant from exchange research program of Italian and Polish Ministries of Education, I.S. acknowledges the Generalitat of Catalunya (2002FI 00667).

### ***5.3.7. References***

<sup>1</sup> Guisnet, M.; Gilson J. P.; eds., *Zeolites for cleaner technologies* Imperial College Press: London, Catalytic Science Series, Vol 3, 2002.

<sup>2</sup> Rege, S. U.; Yang, R. T.; Qian, K.; Buzanowski, M. A.; *Chem. Eng. Sci.* **2001**, 56, 2745.

<sup>3</sup> Castle, W. F. *Int. J. Refrigeration* **2002**, 25, 158.

- <sup>4</sup> Hasegawa, Y.; Watanabe, K.; Kusakabe K.; Morooka, S. *Separ. Purif. Technol.* **2001**, 22-23, 319.
- <sup>5</sup> Giannakopoulos I. G.; Nikolakis, V.; *Ind. Eng. Chem. Res.* **2005**, 44, 226.
- <sup>6</sup> Kobayashi, Y.; Takami, S.; Kubo M.; Miyamoto, A. *Desalination*, **2002**, 147, 339.
- <sup>7</sup> Finnouche, F.; Boucheffa, Y.; Boumaza, R.; Labeled, A.; Magnoux, P. *Ind. Eng. Chem. Res.* **2004**, 43, 6708.
- <sup>8</sup> Vitale G.; Mellot, C. F.; Bull, L. M.; Cheetam, A. K.; *J. Phys. Chem. B* **1997**, 101, 43559.
- <sup>9</sup> Beauvais, C.; Guerrault, X.; Coudert, F. X.; Boutin, A.; Fuchs, A. H. *J. Phys. Chem. B* **2004**, 108, 399
- <sup>10</sup> Davis, R. J. *J. Catal.* **2003**, 216, 396.
- <sup>11</sup> Zecchina, A.; Otero Areán, C. *Chem. Soc. Rev.* **1996**, 25, 187.
- <sup>12</sup> Knözinger, H.; Huber, S. *J. Chem. Soc., Faraday Trans.* **1998**, 94, 2047.
- <sup>13</sup> Hadjiivanov K. I.; Vayssilov, G. N. *Advan. Catal.* **2002**, 47, 307.
- <sup>14</sup> Datka, J.; Gil, B.; Kawalek, M.; Staudte B. *J. Mol. Struct.* **1999**, 511-512, 133.
- <sup>15</sup> Otero Areán, C.; Rodríguez Delgado, M.; Manoilova, O. V.; Turnes Palomino, G.; Tsyganenko A. A.; Garrone E. *Chem. Phys. Lett*, **2002**, 362, 109.
- <sup>16</sup> Onida, B.; Monelli, B.; Borello, L.; Fiorilli, S.; Geobaldo, F.; Garrone, E. *J. Phys. Chem. B* **2002**, 106, 10518.
- <sup>17</sup> Bevilacqua M.; Gutiérrez-Alejandre A.; Resini C.; Casagrande M.; Ramírez J.; Busca, G. *Phys. Chem. Chem. Phys.* **2002**, 4, 4575.
- <sup>18</sup> Bevilacqua, M.; Busca, G. *Catal. Commun.* **2002**, 3, 497.

- <sup>19</sup> Montanari, T.; Bevilacqua, M.; Resini, C.; Busca, G. *J. Phys. Chem. B* **2004**, 108, 2120.
- <sup>20</sup> Lamberti, C.; Bordiga, S.; Geobaldo, F.; Zecchina, A.; Otero-Areán, C.; *J. Chem. Phys.* **1995**, 103, 3158.
- <sup>21</sup> Salla, I.; Salagre, P.; Cesteros, Y.; Medina, F.; Sueiras, J. E.; *J. Phys. Chem. B* **2004**, 108, 5359.
- <sup>22</sup> Maurin, G.; Llewellyn, Ph.; Poyet Th.; Kuchka, B. *J. Phys. Chem. B* **2005**, 109, 125.
- <sup>23</sup> Busca, G.; Ramis, G.; Lorenzelli, V.; Janin, A.; Lavalley, J.C. *Spectrochim. Acta A* **1987**, 43, 489.
- <sup>24</sup> Tielens, F.; Denayer, J. F. M.; Daems, I.; Baron, G. V.; Mortier, W. J.; Geerlings, P. *J. Phys. Chem. B* **2003**, 107, 11065.
- <sup>25</sup> Armaroli, T.; Finocchio, E.; Busca, G. Rossini, S. *Vib. Spectrosc.* **1999**, 20, 85.
- <sup>26</sup> Salla, I.; Montanari, T.; Salagre, P.; Cesteros, Y.; Busca, G.; *J. Phys. Chem. B* **2005**, 109, 915.
- <sup>27</sup> Gilles, F.; Blin, J. L.; Toufar, H.; Briend, M.; Su, B. L.; *Colloids Surf. A Physicochem. Eng. Aspects*, **2004**, 241, 245.
- <sup>28</sup> Bordiga, S.; Scarano, D.; Spoto, G.; Zecchina, A.; Lamberti, C.; Otero Areán, C.; *Vibrational Spectroscopy* **1993**, 5, 69.
- <sup>29</sup> Marra, G. L.; Fitch, A. N.; Zecchina, A.; Ricchiardi, G.; Salvalaggio, M.; Bordiga, S.; Lamberti, C. *J. Phys. Chem. B* **1997**; 101, 10653.
- <sup>30</sup> Vayssilov, G. N.; Staufer, M.; Belling, T.; Neyman, K. M.; Knozinger, H.; Rosch, N. *J. Phys. Chem. B* **1999**; 103; 7920.
- <sup>31</sup> Hüber, S.; Knözinger, H. *Appl. Catal. A: Gen.* **1999**, 181, 239.

- <sup>32</sup> Tsyganenko, A. A.; Escalona Blatero, E.; Otero Areán, C.; Garrone, E.; Zecchina, A. *Catal. Lett.* **1999**, 61, 187.
- <sup>33</sup> Martra, G.; Ocule, R.; Marchese, L.; Centi, G.; Coluccia, S. *Catal. Today* **2002**, 73, 83.
- <sup>34</sup> Shete, B. S.; Kamble, V. S.; Gupta, N. M.; Kartha V. B.; *J. Phys. Chem. B* **1998**, 102, 5581.
- <sup>35</sup> Datka, J.; Boczar, M.; Gil B.; *Colloids Surf. A: Physicoche. Eng. Aspects* **1995**, 105, 1.
- <sup>36</sup> Rege, S. U.; Yang, R.T.; *Chem. Eng. Sci.* **2001**, 56, 3781.
- <sup>37</sup> Angell, C. L.; Howell, M. V. *J. Phys. Chem.* **1969**, 73, 2551.
- <sup>38</sup> Jaramillo, E.; Auerbach, S. M.; *J. Phys. Chem. B.* **1999**, 103, 9589.
- <sup>39</sup> Lim, K. H.; Grey, C. P. *J. Am. Chem. Soc.* **2000**, 122, 9768.
- <sup>40</sup> Buttefey, S.; Boutin, A.; Mellot Draznieks, C.; Fuchs, A. H. *J. Phys. Chem. B* **2001**, 105, 9569.
- <sup>41</sup> Mellot, C. F.; Cheetham, A. K.; *C. R. Acad. Sci. Paris*, **1998**, Série II c, 737.
- <sup>42</sup> Jaramillo, E.; Grey, C. P.; Auerbach, S. M.; *J. Phys. Chem. B* **2001**, 105, 12319.
- <sup>43</sup> Busca, G.; In Metal Oxides: Chemistry and Applications, Fierro, J. L. G.; Ed.; Marcel Dekker Inc Pub., 2005, in press.